

Courant Institute of
Mathematical Sciences

ERDA Mathematics and Computing Laboratory

Green's Function Techniques for the Solution of Time-dependent Potential Flows with a Free Surface in a Bounded Domain

A. Harten and Y. K. Chung

ERDA Research and Development Report

Mathematics and Computers
December 1975

New York University

NEW YORK UNIVERSITY
COURANT INSTITUTE-LIBRARY
251 Mercer St. New York, N.Y. 10012



UNCLASSIFIED

ERDA Mathematics and Computing Laboratory
Courant Institute of Mathematical Sciences
New York University

Mathematics and Computers

C00-3077-100

GREEN'S FUNCTION TECHNIQUES FOR THE SOLUTION OF TIME-DEPENDENT
POTENTIAL FLOWS WITH A FREE SURFACE IN A BOUNDED DOMAIN

A. Harten and Y. K. Chung

Contract No. E(11-1)-3077

UNCLASSIFIED

Abstract

In this report we describe two numerical techniques for the computation of the boundary value of time-dependent potential flows in a bounded domain where part of the boundary is a free surface. The linearized free surface condition relates the normal derivative of the potential to time derivatives of the potential on the undisturbed free surface. It is assumed that on the fixed part of the boundary the normal derivative of the potential is a given function of time.

The problem is formulated via Green's identity. The first technique, QUAKE, uses the classical time-dependent Green's function which satisfies the linearized free surface condition, and the boundary value of the potential is obtained as a solution of an integral equation. The second technique, TDIET, uses the time-independent fundamental solution of the Laplace equation and the boundary value of the potential is obtained as a solution to a differentio-integral equation.

1. Introduction

In this report we consider the following two-dimensional potential flow problem: One or several platforms are floating in a channel; the platforms and the channel are assumed to be infinitely long in the y-direction and to have a uniform and bounded x-z cross-section \hat{C} . The fluid is initially at rest and its motion is generated by the excitation of the confining boundary or the platforms. We assume both the motions of the fluid and the platforms to be small and we approximate the problem by using the two-dimensional transient linear wave theory.

Without loss of generality we assume the boundary Γ of \hat{C} to be composed of coordinate lines with the undisturbed water level at $z = 0$; the flat bottom is located at $z = -H$ (see Fig. 1).

The motion of the fluid, which is assumed irrotational, may be described by means of a velocity potential $\phi(\underline{x}, t)$, $\underline{x} = (x, z)$, satisfying Laplace's equation (see [4], [5])

$$(1.1) \quad \Delta \phi = \phi_{xx} + \phi_{zz} = 0, \quad \underline{x} \in \hat{C}, \quad t > 0$$

and the linearized boundary condition on the undisturbed water surface Γ_F ($z = 0$)

$$(1.2) \quad \phi_{tt}(\underline{x}, t) + g\phi_z = 0, \quad \underline{x} \in \Gamma_F, \quad t > 0.$$

If the free surface is described by $z = Z(x, t)$, then

$$(1.3) \quad Z(x, t) = -\frac{1}{g} \phi_t(x, 0, t).$$

On $\Gamma_A = \Gamma - \Gamma_F$ we require the normal velocity $\frac{\partial}{\partial n} \phi(\underline{x}, t)$ of the fluid to coincide with a given normal velocity of the rigid boundary, i.e.

$$(1.4) \quad \frac{\partial}{\partial n} \phi(\underline{x}, t) = a_n(\underline{x})T(t) , \quad \underline{x} \in \Gamma_A , \quad t \geq 0 .$$

Here $\underline{n} = (n_x, n_z)$ is the unit normal pointing into the domain. The fluid is assumed to start from rest

$$(1.5) \quad Z(\underline{x}, 0) = Z_t(\underline{x}, 0) = 0 , \quad \underline{x} \in \Gamma_F .$$

The pressure $P(x, z, t)$ is determined by a modified form of Euler's integral

$$(1.6) \quad P(\underline{x}, t) + \rho \phi_t + \rho g z = 0 .$$

The term $\frac{1}{2} \rho |\nabla \phi|^2$, being of higher order, has been suppressed; the term $p(\underline{x}, t) = -\rho \phi_t$ is the hydrodynamic pressure.

Our problem, defined by (1.1) - (1.6) can be solved directly by using a finite-difference approximation to the Laplacian operator, (1.1) and the boundary condition, (1.3) (see [1]). However in many engineering problems only the solution on the boundary, namely the wave-height (1.3) as well as the pressure exerted on the floating platforms and the confining walls, is of interest. Thus only the solution of the boundary potential need be obtained; a method based on Green's identity is tailored for this situation. Sometimes it is convenient to solve directly for the acceleration potential $\psi = \phi_t$. In terms of the acceleration potential, the free surface elevation (1.3) is given by

$$(1.7) \quad Z(\underline{x}, t) = -\frac{1}{g} \psi(\underline{x}, 0, t)$$

and the hydrodynamic pressure is given by

$$(1.8) \quad p(\underline{x}, t) = -\rho\psi(\underline{x}, t) .$$

It is easy to verify that ψ satisfies Laplace's equation and the following boundary conditions which are analogous to (1.2) and (1.4):

$$(1.9) \quad \psi_{tt}(\underline{x}, t) + g\psi_z(\underline{x}, t) = 0 , \quad \underline{x} \in \Gamma_F , \quad t > 0 ,$$

$$(1.10) \quad \frac{\partial}{\partial n} \psi(\underline{x}, t) = a_n(\underline{x}) \dot{T}(t) , \quad \underline{x} \in \Gamma_A , \quad t \geq 0$$

where

$$\dot{T}(t) = \frac{d}{dt} T(t) .$$

We shall now describe two numerical techniques for the computation of the boundary potential. In Section 2 we shall describe QUAKE, which is a technique based on the particular choice of the classical time-dependent Green's function; this choice results in an integral equation for the boundary potential. QUAKE is applicable to open sea problems (unbounded domain) as well. In Section 3 we shall describe TDIET which is based on a particular choice of a Green's function which is independent of time; this choice results in an integro-differential equation for the boundary potential. In its present form TDIET is applicable only to problems in a bounded domain. In this case it is much more efficient than QUAKE and the finite-difference methods in [1].

Both QUAKE and TDIET are easily extendible to domains with curved boundaries and to problems with a three-dimensional geometry.

In Section 4 we present some numerical results.

$$(1.7) \quad Z(\underline{x}, t) = - \frac{1}{g} \psi(\underline{x}, 0, t)$$

and the hydrodynamic pressure is given by

$$(1.8) \quad p(\underline{x}, t) = -\rho\psi(\underline{x}, t) \ .$$

It is easy to verify that ψ satisfies Laplace's equation and the following boundary conditions which are analogous to (1.2) and (1.4):

$$(1.9) \quad \psi_{tt}(\underline{x}, t) + g\psi_z(\underline{x}, t) = 0 \ , \quad \underline{x} \in \Gamma_F \ , \quad t > 0 \ ,$$

$$(1.10) \quad \frac{\partial}{\partial n} \psi(\underline{x}, t) = a_n(\underline{x})\dot{T}(t) \ , \quad \underline{x} \in \Gamma_A \ , \quad t \geq 0$$

where

$$\dot{T}(t) = \frac{d}{dt} T(t) \ .$$

We shall now describe two numerical techniques for the computation of the boundary potential. In Section 2 we shall describe QUAKE, which is a technique based on the particular choice of the classical time-dependent Green's function; this choice results in an integral equation for the boundary potential. QUAKE is applicable to open sea problems (unbounded domain) as well. In Section 3 we shall describe TDIET which is based on a particular choice of a Green's function which is independent of time; this choice results in an integro-differential equation for the boundary potential. In its present form TDIET is applicable only to problems in a bounded domain. In this case it is much more efficient than QUAKE and the finite-difference methods in [1].

Both QUAKE and TDIET are easily extendible to domains with curved boundaries and to problems with a three-dimensional geometry.

In Section 4 we present some numerical results.

2. Time-dependent Green's Function Method (QUAKE)

Let $G(\underline{x}, \underline{\xi}, t)$, $\underline{x} = (x, z)$, $\underline{\xi} = (\xi, \zeta)$, be a time-dependent Green's function which satisfies the following:

$$(2.1a) \quad G(\underline{x}, \underline{\xi}, t) = \log R + W(\underline{x}, \underline{\xi}, t)$$

where

$$R^2 = (x - \xi)^2 + (z - \zeta)^2 ,$$

$$(2.1b) \quad \Delta_{\underline{x}} W = 0 , \quad \text{for } \underline{x} \in \mathcal{U} \text{ and } t > 0$$

$$(2.2) \quad G_{tt} + gG_z = 0 , \quad \text{for } \underline{\xi} \in \Gamma_F \text{ and } t > 0$$

$$(2.3) \quad G_z = 0 , \quad \text{at } \zeta = -H \text{ and for } t > 0$$

$$(2.4a) \quad G(\underline{x}, \underline{\xi}, t) = G(\underline{x}, \underline{\xi}, -t) , \quad \text{for all } t$$

$$(2.4b) \quad G(\underline{x}, \underline{\xi}, 0) = 0 , \quad \text{for } \underline{\xi} \in \Gamma_F .$$

Such $G(\underline{x}, \underline{\xi}, t)$ exists and is given explicitly by the following expression:

$$(2.5a) \quad G = \log (R/R') - 2 \int_0^\infty \frac{e^{-KH} \sinh (Kz) \sinh (K\zeta) \cos (Kr) dK}{K \cosh (KH)} \\ - 2 \int_0^\infty \frac{\cosh K(z+H) \cosh K(\zeta+H) [1 - \cos (\omega t)]}{K \cosh^2 (KH) \tanh (KH)} \cos (Kr) dK$$

where

$$(2.5b) \quad \omega^2 = gK \tanh (KH) , \quad R' = [(x - \xi)^2 + (z + \zeta)^2]^{\frac{1}{2}} , \quad r = |x - \xi| .$$

(See [2], [4] and [5].) Observe that, as one expects, $G(\underline{x}, \underline{\xi}, t)$ is symmetric in \underline{x} and $\underline{\xi}$.

In order to derive an integral equation, we apply Green's theorem to the functions $\psi(\underline{x}, t)$ and $G(\underline{x}, \underline{\xi}, t-\tau)$ (see [5])

$$(2.6) \quad 2\pi\psi(\underline{x}, t) = \oint_{\Gamma} [G(\underline{x}, \underline{\xi}, t-\tau)\psi_n(\underline{\xi}, t) - G_n(\underline{x}, \underline{\xi}, t-\tau)\psi(\underline{\xi}, t)] ds_{\xi} \\ \text{for all } \underline{x} \in D \quad .$$

Integrating (2.6) with respect to t between $t = 0$ and $t = \tau$ we find

$$(2.7) \quad 2\pi[\phi(\underline{x}, \tau) - \phi(\underline{x}, 0)] = \int_0^{\tau} \oint_{\Gamma} [G(\underline{x}, \underline{\xi}, t-\tau)\psi_n(\underline{\xi}, t) \\ - G_n(\underline{x}, \underline{\xi}, t-\tau)\psi(\underline{\xi}, t)] ds_{\xi} dt \quad .$$

We observe that because of the boundary conditions (1.9) and (2.2), the integrand on Γ_F in (2.7) can be written as the following time derivative

$$G\psi_n - \psi G_n = \frac{1}{g} (G\psi_{tt} - \psi G_{tt}) = \frac{1}{g} \frac{\partial}{\partial t} (G\psi_t - \psi G_t) \quad .$$

Using this relation together with (1.5) and (2.4), we get

$$(2.8) \quad \int_0^{\tau} \int_{\Gamma_F} [G(\underline{x}, \underline{\xi}, t-\tau)\psi_n(\underline{\xi}, t) - G_n(\underline{x}, \underline{\xi}, t-\tau)\psi(\underline{\xi}, t)] ds_{\xi} \\ = \frac{1}{g} \int_{\Gamma_F} \{ [G(\underline{x}, \underline{\xi}, 0)\psi_t(\underline{\xi}, \tau) - G_t(\underline{x}, \underline{\xi}, 0)\psi(\underline{\xi}, \tau)] \\ - [G(\underline{x}, \underline{\xi}, \tau)\psi_t(\underline{\xi}, 0) - G_t(\underline{x}, \underline{\xi}, \tau)\psi(\underline{\xi}, 0)] \} ds_{\xi} = 0 \quad .$$

Thus the integral in (2.7) can be only taken along $\Gamma_A = \Gamma - \Gamma_F$. Substituting for ψ_n on Γ_A the values (1.10), we obtain

$$(2.9) \quad 2\pi[\dot{\phi}(\underline{x}, \tau) - \dot{\phi}(\underline{x}, 0)] = \int_0^\tau \int_{\Gamma_A} [G(\underline{x}, \underline{\xi}, t-\tau) a_n(\underline{\xi}) \dot{T}(t) - G_n(\underline{x}, \underline{\xi}, t-\tau) \psi(\underline{\xi}, t)] ds_\xi dt .$$

Now we differentiate equation (2.9) with respect to τ and use the relations $G_t = -G_\tau$, $G_{nt} = -G_{n\tau}$ and (2.4)

$$(2.10) \quad 2\pi\psi(\underline{x}, \tau) = \int_{\Gamma_A} [G(\underline{x}, \underline{\xi}, 0) a_n(\underline{\xi}) \dot{T}(\tau) - G_n(\underline{x}, \underline{\xi}, 0) \psi(\underline{\xi}, \tau)] ds_\xi + \int_0^\tau \int_{\Gamma_A} [G_{nt}(\underline{x}, \underline{\xi}, t-\tau) \psi(\underline{\xi}, t) - G_t(\underline{x}, \underline{\xi}, t-\tau) a_n(\underline{\xi}) \dot{T}(t)] ds_\xi dt .$$

Next we let $\underline{x} \in \mathcal{L}$ in (2.10) approach a point on the boundary Γ_A . This results in the following integral equation for the boundary potential:

$$(2.11a) \quad \lambda(\underline{x})\psi(\underline{x}, \tau) + \text{P.V.} \int_{\Gamma_A} G_n(\underline{x}, \underline{\xi}, 0) \psi(\underline{\xi}, \tau) ds_\xi = \int_0^\tau \int_{\Gamma_A} G_{nt}(\underline{x}, \underline{\xi}, t-\tau) \psi(\underline{\xi}, t) ds_\xi dt + c(\underline{x}, \tau) ,$$

$$(2.11b) \quad c(\underline{x}, \tau) = - \int_{\Gamma_A} G(\underline{x}, \underline{\xi}, 0) a_n(\underline{\xi}) \dot{T}(\tau) ds_\xi + \int_0^\tau [\dot{T}(t) \int_{\Gamma_A} G_t(\underline{x}, \underline{\xi}, t-\tau) a_n(\underline{\xi}) ds_\xi] dt .$$

Here P.V. indicates the Cauchy principal value integral and $\lambda(\underline{x})/2\pi$ is the part of an infinitesimal circle centered at the boundary point \underline{x} , which is contained in \mathcal{L} .

The convolution with respect to time in the right-hand side of (2.11) is approximated by some quadrature formula, e.g. the trapezoidal rule:

$$\begin{aligned} \int_0^\tau \int_{\Gamma_A} G_{nt}(\underline{x}, \underline{\xi}, t-\tau) \psi(\underline{\xi}, t) ds_\xi dt &\approx \frac{\Delta t}{2} \int_{\Gamma_A} G_{nt}(\underline{x}, \underline{\xi}, 0) \psi(\underline{\xi}, \tau) ds_\xi \\ &+ \Delta t \sum_{\ell=1}^{L-1} \int_{\Gamma_A} G_{nt}(\underline{x}, \underline{\xi}, \ell \Delta t) \psi(\underline{\xi}, (L-\ell) \Delta t) ds_\xi \end{aligned}$$

where $L = \tau/\Delta t$.

Next we discretize (2.11) with respect to space by dividing the boundary Γ_A into intervals Δ_i , $1 \leq i \leq N_A$. QUAKE uses a piecewise constant approximation to ψ ; the constant values are $\psi_i^\ell = \psi(\underline{x}_i, \ell \Delta t)$ where \underline{x}_i is the center of Δ_i .

With this discretization (2.11) becomes a system of N linear equations

$$(2.12) \quad A \underline{\psi}^L = \Delta t \sum_{\ell=1}^{L-1} B^\ell \underline{\psi}^{L-\ell} + \gamma^L$$

where

$$\underline{\psi}^\ell = \begin{pmatrix} \psi_1^\ell \\ \vdots \\ \psi_N^\ell \end{pmatrix}$$

and A is an $N_A \times N_A$ constant matrix whose entries are

$$(2.13a) \quad A_{ij} = \delta_{ij} \lambda(\underline{x}_i) + \text{P.V.} \int_{\Delta_j} G_n(\underline{x}_i, \underline{\xi}, 0) ds_\xi - \frac{\Delta t}{2} \int_{\Delta_j} G_{nt}(\underline{x}_i, \underline{\xi}, 0) ds_\xi$$

B^ℓ is an $N_A \times N_A$ matrix whose entries are

$$(2.13b) \quad B_{i,j}^{\ell} = \int_{\Delta_j} G_{nt}(\underline{x}_i, \underline{\xi}, \ell \Delta t) ds_{\underline{\xi}}$$

$\underline{\gamma}^L$ is an N_A vector whose components are

$$(2.14a) \quad \gamma_i^L = c(\underline{x}_i, L\Delta t) = -\alpha_i \dot{T}(L\Delta t) - \frac{\Delta t}{2} [\dot{T}(0)\beta_i^L + \dot{T}(L\Delta t)\beta_i^0] \\ - \Delta t \sum_{\ell=1}^{L-1} \dot{T}((L-\ell)\Delta t)\beta_i^{\ell}$$

where we have introduced

$$(2.14b) \quad \alpha_i = \int_{\Gamma_A} G(\underline{x}_i, \underline{\xi}, 0) a_n(\underline{\xi}) ds_{\underline{\xi}} ,$$

$$(2.14c) \quad \beta_i^{\ell} = \int_{\Gamma_A} G_t(\underline{x}_i, \underline{\xi}, \ell \Delta t) a_n(\underline{\xi}) ds_{\underline{\xi}} .$$

We observe that the matrix A and the vector $\underline{\alpha}$ are independent of time and therefore have to be computed only once. The number of operations needed to compute L time-steps of the potential on Γ_A is proportional to $L^2 N_A^3$. The quadratic dependence on the number of time steps is due to the need to evaluate the convolution integral in (2.11). Obviously QUAKE requires a large memory allocation because of this convolution. If the free surface potential is needed, then an additional computing time has to be expected.

QUAKE can handle unbounded domains as well as bounded domains. In fact, it is less costly for unbounded domains than for a corresponding problem in a bounded domain.

3. TDIET (Time-dependent Differentio-Integral Equation Technique)

Let $G(\underline{x}, \underline{\xi})$ be the following time-independent Green's function

$$(3.1) \quad G(\underline{x}, \underline{\xi}) = \log R + W(\underline{x}, \underline{\xi})$$

where R is defined in (2.5b) and $W(\underline{x}, \underline{\xi})$ is any function which is harmonic for all $\underline{x} \in \mathcal{L}'$. $\psi(\underline{x}, t)$ satisfies Laplace's equation in \mathcal{L}' for all $t > 0$. Therefore, the following Green's identity is satisfied for all $t > 0$

$$(3.2) \quad \lambda(\underline{x}) \psi(\underline{x}, t) = \oint_{\Gamma} [G(\underline{x}, \underline{\xi}) \frac{\partial}{\partial n} \psi(\underline{\xi}, t) - \psi(\underline{\xi}, t) \frac{\partial}{\partial n} G(\underline{x}, \underline{\xi})] ds_{\xi}$$

where $\lambda(\underline{x})/2\pi$ is the part of an infinitesimal circle centered at \underline{x} which is contained in \mathcal{L}' . Substituting the boundary conditions (1.9) and (1.10) for $\frac{\partial \psi}{\partial n}$ in (3.2) results in the following integro-differential equation

$$(3.3) \quad \lambda(\underline{x}) \psi(\underline{x}, t) + \oint_{\Gamma} \psi(\underline{\xi}, t) \frac{\partial}{\partial n} G(\underline{x}, \underline{\xi}) ds_{\xi} \\ + \frac{1}{g} \int_{\Gamma_F} G(\underline{x}, \underline{\xi}) \psi_{tt}(\underline{\xi}, t) ds_{\xi} = \dot{T}(t) \int_{\Gamma_A} G(\underline{x}, \underline{\xi}) a_n(\underline{\xi}) ds_{\xi} .$$

A convenient choice of a Green's function is one for which $\frac{\partial}{\partial n} G(\underline{x}, \underline{\xi}) = 0$ for $\underline{\xi} \in \Gamma_A$. In this case, the second integral on the left-hand side of (3.3) is taken only along Γ_F and the resulting discretization leads to a linear system of ordinary differential equations

$$(3.4) \quad A \frac{d^2}{dt^2} \underline{\psi}_F(t) + B \underline{\psi}_F(t) = \underline{a}(t)$$

for the N_F discrete values of the potential ψ along the free surface Γ_F ; A and B are $N_F \times N_F$ matrices. After obtaining an approximation $\tilde{\psi}_F(\underline{x}, t)$ for the potential on Γ_F by solving (3.4) as an initial value problem, the approximate solution $\tilde{\psi}_A(\underline{x}, t)$ for the potential on $\Gamma_A = \Gamma - \Gamma_F$ is obtained from solving (3.3) with $G(\underline{x}, \underline{\xi}) = \log R$.

$$\begin{aligned}
 (3.5) \quad \dot{\psi}(\underline{x}) \tilde{\psi}_A(\underline{x}, t) + \int_{\Gamma_A} \tilde{\psi}_A(\underline{\xi}, t) \frac{\partial}{\partial n} \log R \, ds_{\xi} \\
 = \dot{\Gamma}(t) \int_{\Gamma_A} \log R \cdot a_n(\underline{\xi}) ds_{\xi} - \int_{\Gamma_F} [\tilde{\psi}_F(\underline{\xi}, t) \frac{\partial}{\partial n} \log R \\
 + \frac{1}{\varepsilon} \log R \cdot \frac{\partial^2}{\partial t^2} \psi_F(\underline{\xi}, t)] ds_{\xi} .
 \end{aligned}$$

The right-hand side of (3.5) is known and therefore the discretization of (3.5) leads to the following system of linear equations

$$(3.6) \quad C \cdot \underline{\psi}_A(t) = \underline{b}(t)$$

for the N_A discrete values of the potential along Γ_A ; the $N_A \times N_A$ matrix, C , is independent of time.

This approach cannot be implemented directly in a numerical code since an explicit expression for $G(\underline{x}, \underline{\xi})$ such that $\frac{\partial}{\partial n} G(\underline{x}, \underline{\xi}) = 0$ for $\underline{\xi} \in \Gamma_A$, is not always available. In the following we shall present a technique to arrive at (3.4) and (3.6) without requiring an explicit form of the Green's function. The main idea in TDIET is to first discretize (3.3) with $G(\underline{x}, \underline{\xi}) = \log R$ and then to obtain the desired decomposition by an ordered elimination procedure.

(i) Discretization: Let \underline{x}_j , $1 \leq j \leq N$, be a partition of the boundary and let $\psi_j(t) = \psi(\underline{x}_j, t)$. It is convenient to order the partition points so that \underline{x}_j , $1 \leq j \leq N_A$, are the points along Γ_A and \underline{x}_j , $N_A+1 \leq j \leq N$, are points along the free surface Γ_F ; $N_F = N - N_A$. We denote by $S_j(\underline{x})$ the unit cubic spline such that

$$(3.7) \quad S_j(\underline{x}_i) = \delta_{ij} \quad (\delta_{ij} = 0 \text{ for } i \neq j, \quad \delta_{ij} = 1 \text{ for } i = j) .$$

In the particular geometry of Figure 1, the boundary has corners. We construct $S_j(\underline{x})$ so that it will be continuous up to the second derivative in a linear segment which includes \underline{x}_j and to be identically zero in all other segments. This way, the approximations

$$(3.8a) \quad \psi(\underline{x}, t) \sim \sum_{j=1}^N S_j(\underline{x}) \psi_j(t) ,$$

$$(3.8b) \quad \psi_{tt}(\underline{x}, t) \sim \sum_{j=1}^N S_j(\underline{x}) \frac{d^2}{dt^2} \psi_j(t)$$

are continuous up to the second derivative, except at the corner points where only continuity of the function is assumed. Because of the singular nature of the corners, the partition points are so distributed that $|\Delta \underline{x}_j| = |\underline{x}_{j+1} - \underline{x}_j|$ is smaller in the neighborhood of the corners.

Next, equation (3.3) is discretized by using the cubic spline approximation (3.8)

$$\begin{aligned} (3.3) \quad \lambda(\underline{x}_1) \mu_1(t) &+ \sum_{j=1}^N \psi_j(t) \int_{\Gamma} S_j(\underline{\xi}) \frac{\partial}{\partial n} G(\underline{x}_1, \underline{\xi}) dS_{\xi} \\ &+ \frac{1}{\varepsilon} \sum_{j=N_A+1}^N \frac{d^2}{dt^2} \psi_j(t) \int_{\Gamma_F} S_j(\underline{\xi}) G(\underline{x}_1, \underline{\xi}) dS_{\xi} \\ &= \dot{T}(t) \int_{\Gamma_A} G(\underline{x}_1, \underline{\xi}) a_n(\underline{\xi}) dS_{\xi} \quad , \quad 1 \leq i \leq N \quad . \end{aligned}$$

The N equations (3.3) can be written in the following matrix form

$$(3.10) \quad E_{\bullet,1}(t) = \dot{T}(t) \underline{a}$$

where \underline{u} is an $N+N_F$ vector whose components are

$$(3.11) \quad u_i(t) = \begin{cases} \psi_A(\underline{x}_i, t) & , \quad 1 \leq i \leq N_A \\ \frac{\partial^2}{\partial t^2} \psi_F(\underline{x}_i, t) & , \quad N_A+1 \leq i \leq N \\ \psi_F(\underline{x}_{i-N_F}, t) & , \quad N+1 \leq i \leq N+N_F \end{cases}$$

$\mathbf{a}(t)$ is an N vector the components of which are

$$(3.12) \quad a_i = \int_{\Gamma_A} G(\underline{x}_i, \underline{s}) a_n(\underline{s}) ds_{\underline{s}}, \quad 1 \leq i \leq N$$

E is an $N \times (N + N_F)$ matrix whose entries are

$$(3.13a) \quad E_{ij} = \lambda(\underline{x}_i) \delta_{ij} + \int_{\Gamma} S_j(\underline{\xi}) \frac{\partial}{\partial n} G(\underline{x}_i, \underline{\xi}) d s_{\xi} \quad , \quad 1 \leq i \leq N \quad , \\ 1 \leq j \leq N_A \quad ,$$

$$(3.13b) \quad E_{ij} = \frac{1}{g} \int_{\Gamma_F} S_j(\underline{\xi}) G(\underline{x}_i, \underline{\xi}) dS_{\underline{\xi}} \quad , \quad 1 \leq i \leq N \quad , \quad N_A+1 \leq j \leq N \quad ,$$

$$(3.13) \quad \varphi_{i,j} = \lambda(\underline{x}_i) \varphi_{i,j-N_F} + \int_{\Gamma} \varphi_{j-N_F}(\underline{x}) \frac{\partial}{\partial n} G(\underline{x}, \underline{\xi}) d\Gamma_{\underline{\xi}}, \\ 1 \leq i \leq N, \quad 1+2 \leq j \leq N+N_F.$$

We observe that $\varphi_{i,j}$, $1 \leq i \leq N$, $1 \leq j \leq N+N_F$, as well as a_i , $1 \leq i \leq N$, depend only on the geometry of the boundary and are independent of time, provided that the Green's function is independent of time. As was mentioned earlier, we choose $G(\underline{x}, \underline{\xi}) = \log R$, $R^2 = (x-\xi)^2 + (z-\zeta)^2$, for an arbitrarily shaped domain. In case the bottom is flat as in Figure 1, we take $G(\underline{x}, \underline{\xi}) = \log R\hat{R}$, $\hat{R}^2 = (x-\xi)^2 + (z+\zeta+2H)^2$. This way $\frac{\partial}{\partial n} G(\underline{x}, \underline{\xi}) = 0$ on the flat bottom $\zeta = -H$. Therefore the integrand in the integrals in (3.13) is identically zero on the bottom, and the potential values on the bottom are eliminated from the equations (3.10)-(3.13).

We remark that in the particular geometry of Figure 1, where the boundary is composed of coordinate lines, the coefficients (3.12)-(3.13) may be computed analytically. This is needed, at least locally, because of the singularity of the integrand at $\underline{x}_i = \underline{\xi}$ (see [7]).

11. Solution of the discrete problem: In order to obtain an analog to the equations (3.4) and (3.6), a Gauss elimination (with row pivoting) is applied to the matrix equation (3.10). The unknowns $\varphi_1, \dots, \varphi_{N-1}$ are eliminated from the j -th equation, $1 \leq j \leq N$. The resulting matrix equation is of the following form

$$\begin{array}{c}
 \leftarrow N_A \rightarrow \quad \leftarrow N_F \rightarrow \quad \leftarrow N_F \rightarrow \\
 \downarrow N_A \quad \downarrow N_F \\
 (3.14) \quad \begin{bmatrix} U_A & & \\ C & Q & R \\ & U_F & S \end{bmatrix} \begin{bmatrix} \underline{\psi}_A(t) \\ \underline{\psi}_F(t) \\ \underline{\psi}_F(t) \end{bmatrix} = \begin{bmatrix} \underline{c}_A \\ \underline{c}_F \end{bmatrix} \cdot \dot{T}(t)
 \end{array}$$

The last N_F equations

$$(3.15) \quad U_F \frac{d^2}{dt^2} \underline{\psi}_F(t) + S \underline{\psi}_F(t) = \underline{c}_F \frac{d}{dt} T(t)$$

comprise a system of linear ordinary differential equations similar to (3.4); U_F is an upper diagonal matrix. This subproblem for the discrete values of the potential on the free surface is now solved independently as an initial value problem in the time interval of interest. The initial value problems (3.15) and (1.5) can be solved numerically by any standard method; our computer code uses a fourth order accurate method of Runge-Kutta.

Once the free surface potential $\underline{\psi}_F(t)$ has been computed in the time interval of interest, $\underline{\psi}_A(t)$ can be found at the desired time-levels by solving the system composed of the first N_A linear equations in (3.14)

$$(3.16) \quad U_A \underline{\psi}_A(t) = \frac{d}{dt} T(t) \underline{c}_A - Q \frac{d^2}{dt^2} \underline{\psi}_F(t) - R \underline{\psi}_F(t) .$$

Observe that U_A is an upper diagonal matrix. Hence, once the right-hand side of (3.16) is computed, the solution $\underline{\psi}_A(t)$ is obtained by a simple back substitution.

In its present form, TDIET is applicable for problems in a bounded domain where only the boundary potential is needed. In case the potential is needed for a few time levels in the domain, it still is efficient to use TDIET to compute the boundary potential at the desired time levels and then to solve a Dirichlet problem.

We have described TDIET for two dimensional computations. For the formulation in three dimensions one has only to change the Green's function and the notation.

4. Numerical results

In this section we shall present several numerical results which will demonstrate the efficiency and the accuracy of TDIET.

(i) Free surface disturbances

We consider an empty rectangular basin $0 \leq x \leq 2L$, $-H \leq z \leq 0$, in which the confining walls and the bottom are at rest.

$$(4.1) \quad \phi_x(0, z, t) = \phi_x(2L, z, t) = \phi_z(x, -H, t) = 0, \quad t \geq 0.$$

The motion of the fluid is generated by initially disturbing the free surface

$$(4.2a) \quad \phi(x, 0, 0) = I(x) = \sum_{n=0}^{\infty} I_n \cos \frac{n\pi}{L} x,$$

$$(4.2b) \quad \phi_t(x, 0, 0) = J(x) = \sum_{n=0}^{\infty} J_n \cos \frac{n\pi}{L} x$$

or by applying a periodic pressure impulse to the free surface

$$(4.2c) \quad P(x, t) = p(x) \sin \Omega t = \sin \Omega t \sum_{n=0}^{\infty} P_n \cos \frac{n\pi}{L} x.$$

The free surface condition (1.6) becomes

$$(4.3) \quad \phi_{tt} + g\phi_z = -\frac{1}{\rho} P_t(x, t) = -\frac{\Omega}{\rho} p(x) \cos \Omega t$$

and a corresponding inhomogeneous term is added to the system of the ordinary differential equations (3.10).

It is easily verified that the solution to the problem (4.1)-(4.2) is

$$\begin{aligned}
(4.4a) \quad \phi(x, z, t) = & \sum_{n=0}^{\infty} I_n \frac{\cosh \frac{n\pi}{L} (z+H)}{\cosh \frac{n\pi}{L} H} \cos \frac{n\pi}{L} x \cos \omega_n t \\
& + J_0 t + \sum_{n=1}^{\infty} J_n \frac{\cosh \frac{n\pi}{L} (z+H)}{\omega_n \cosh \frac{n\pi}{L} H} \cos \frac{n\pi}{L} x \sin \omega_n t \\
& + \frac{\Omega}{\rho} \sum_{n=0}^{\infty} P_n \frac{\cos \Omega t - \cos \omega_n t}{\Omega^2 - \omega_n^2} \frac{\cosh \frac{n\pi}{L} (z+H)}{\cosh \frac{n\pi}{L} H} \cos \frac{n\pi}{L} x,
\end{aligned}$$

$$\begin{aligned}
(4.4b) \quad Z(x, t) = & -\frac{J_0}{g} + \frac{1}{g} \sum_{n=1}^{\infty} \cos \frac{n\pi}{L} x (I_n \omega_n \sin \omega_n t - J_n \cos \omega_n t) \\
& + \frac{\Omega}{\rho} P_n \frac{\Omega \sin \Omega t - \omega_n \sin \omega_n t}{\Omega^2 - \omega_n^2}
\end{aligned}$$

where

$$(4.4c) \quad \alpha_n = \frac{n\pi}{L}, \quad \omega_n^2 = g \alpha_n \tanh \alpha_n H.$$

Example 1: Initial evaluation

$$(4.5a) \quad \phi(x, 0, 0) = 0,$$

$$\begin{aligned}
(4.5b) \quad \phi_t(x, 0, 0) = & 10 \sum_{n=0}^{49} \frac{1}{(2n+1)^2} \cos \left[(2n+1)\pi \frac{x+100}{100} \right] \\
\approx & \begin{cases} -\frac{\pi^2}{40} (x+50), & -100 \leq x \leq 0 \\ -\frac{\pi^2}{40} (50-x), & 0 \leq x \leq 100 \end{cases}.
\end{aligned}$$

$$(4.5c) \quad P(x, t) \equiv 0.$$

The initial free surface elevation is shown in Fig. 2a; 25 points are equally distributed along the undisturbed free surface $z = 0$, $-100 \leq x \leq 100$. The depth is $H = 10$. This problem is

$0 \leq t \leq 10$, and $0 \leq x \leq 100$. The initial conditions are $z(x, 0) = 0$, $z(x, 10) = 0$, and $z(0, t) = 0$, $z(100, t) = 0$. The boundary conditions are $z(0, t) = 0$, $z(100, t) = 0$. The time step is $\Delta t = 0.1$. The spatial step is $\Delta x = 1$. The relative error is 1.39% .

$$(4.69) \quad \text{Error} = \frac{\sum_{i=1}^N |z_i^{\text{num}} - z_i^{\text{exact}}|^2}{\sum_{i=1}^N |z_i^{\text{exact}}|^2} = 0.42\%$$

$$(4.70) \quad \text{Error} = \frac{\sum_{i=1}^N |z_i^{\text{num}} - z_i^{\text{exact}}|^2}{\sum_{i=1}^N |z_i^{\text{exact}}|^2} = 1.39\%$$

The CPU time on the CDC 6600 for this computation is 3.85 seconds: 2.32 seconds to arrive at the discrete formulation and 1.53 seconds to advance the solution in 50 time steps.

Example 2: Particle in a magnetic field

$$(4.71) \quad p(x, t) = \begin{cases} 0 & \text{for } x < 0 \\ 1 & \text{for } 0 \leq x \leq 100 \end{cases}$$

$$(4.72) \quad p(x, t) = \begin{cases} 0 & \text{for } x < 0 \\ 1 & \text{for } 0 \leq x \leq 100 \end{cases}$$

$$(4.73) \quad p(x) = \frac{1}{100} + \frac{1}{100} \sum_{n=1}^{\infty} \left[\left(\frac{1}{n} - \alpha^2 \pi^2 \right) \sin(n\pi x) - \frac{1}{n} \cos(n\pi x) \right] \frac{(-1)^n}{n^2} \cos(n\pi \frac{x+100}{100})$$

$$\approx \begin{cases} \left(\left(\frac{x}{100\alpha} \right)^2 - 1 \right)^2, & |x| \leq 100\alpha \\ 0, & |x| \geq 100\alpha \end{cases}$$

$p(x)$ given by (4.73) with $\alpha = 0.25$ is shown in Figure 3a. The geometry in this example is identical to the one in Example 1. This problem is solved for $0 \leq t \leq 10$ (2 periods), using 80 time

steps. Figures 2b, 2c, 2d and 2e show the calculated free surface elevation (the continuous line) and the exact free surface elevation (4.4b) (asterisks) at $t = 2.5, 5., 7.5, 10.,$ respectively. The relative L_2 -errors (4.6) at $t = 10$ are $e(\phi) = 0.425\%$ and $e(Z) = 0.614\%$. The CP time on the CDC 6600 for this calculation is 4.8 seconds: 2.4 seconds to arrive at the discrete formulation and 2.4 seconds to advance the solution in 80 time steps.

(ii) Harmonic excitation of walls

We consider an empty rectangular basin $0 \leq x \leq 2L,$
 $-H \leq z \leq 0,$ in which the bottom is at rest and the free surface is undisturbed.

$$(4.6a) \quad \phi(x, 0, 0) = \phi_t(x, 0, 0) = 0, \quad 0 \leq x \leq 2L,$$

$$(4.6b) \quad P(x, t) = \phi_z(x, -H, t) = 0, \quad 0 \leq x \leq 2L, \quad t \geq 0.$$

The motion of the fluid is generated by applying harmonic excitation to the walls

$$(4.7) \quad \phi_x(0, z, t) = \phi_x(2L, z, t) = -A \cos \Omega t, \quad -H \leq z \leq 0, \quad t \geq 0.$$

The solution to this problem can be approximated by the following expression

$$(4.8a) \quad \phi(x, z, t) = \frac{4A}{L} \cos \Omega t \sum_{k=0}^{\infty} \alpha_{2k+1}^{-2} \left[1 - \frac{\Omega^2}{\Omega^2 - \omega_{2k+1}^2} \frac{\cosh \alpha_{2k+1}(z+H)}{\cosh \alpha_{2k+1}H} \right] \cos(\alpha_{2k+1}x) \\ + \frac{4A}{L} \sum_{k=0}^{\infty} \alpha_{2k+1}^{-2} \frac{\omega_{2k+1}^2}{\Omega^2 - \omega_{2k+1}^2} \frac{\cosh \alpha_{2k+1}(z+H)}{\cosh \alpha_{2k+1}H} \cos \alpha_{2k+1}x \cos \omega_n t$$

where α_k and ω_k are given by (4.4b). The free surface elevation is given by the following expression

$$(4.8b) \quad Z(x,t) = \frac{4A}{gL} \Omega \sin \Omega t \sum_{k=0}^{\infty} \alpha_{2k+1}^{-2} \left[1 - \frac{\Omega^2}{\Omega^2 - \omega_{2k+1}^2} \right] \cos \alpha_{2k+1} x \\ + \frac{4A}{gL} \sum_{k=0}^{\infty} \alpha_{2k+1}^{-2} \frac{\omega_{2k+1}^3}{\Omega^2 - \omega_{2k+1}^2} \cos \alpha_{2k+1} x \sin \omega_{2k+1} t .$$

Figure 4 shows a comparison between (4.8b) and the solution of TDIET with $\Omega = 2\pi$ at $t = 0.75$. The geometry of the basin is given in the figure.

(iii) Heaving of a rectangular cylinder

In this example we compute the forced heaving motion of a semi-submerged rectangular cylinder in the free surface. As in [1] we choose a rectangular cylinder with a draft $D = 1$ and a beam $B = 2$; the water depth is $H = 7.15$ (see Fig. 1). The vertical velocity of the cylinder is

$$(4.9) \quad \phi_z(x, -D, t) = 0.1 \Omega \cos \Omega t, \quad \Omega = 1.253 \sqrt{g} .$$

In order to simulate open sea conditions, the walls are placed at $x = \pm 16$. Although the solution is symmetric in x we solve the complete problem. Each of the free surface segments $1 \leq |x| \leq 16$ is divided into 24 unequal intervals, the size of which increases quadratically with $|x|$. The bottom of the cylinder is divided into 12 intervals. The sides of the cylinder and the walls are each divided into 8 intervals.

Figures 5a, 5b and 5c show the wave profile at the end of 1, 2, and three oscillations of the cylinder, respectively.

Observe the establishment of a standing wave pattern near the body and that the asymptotic wave length $\lambda_{\infty} = 2\pi g/\Omega^2 = 4$ is almost reached. These wave profiles, although qualitatively similar, are not identical to those shown in [1]; this is probably due to different initialization of the problem. However, the dynamic pressure force agrees quite well with the results reported in [1].

The CP time on the CDC 6600 for this calculation is 23 seconds: 12 seconds to set up the discrete formulation and 11 seconds to advance the solution in 90 time steps (30 time steps per oscillation).

(iv) Seismic excitation of a rectangular cylinder

In this last example we compute the forces exerted on a semi-submerged rectangular cylinder which is held fixed in the fluid. The horizontal confining walls are excited by an acceleration which resembles earthquakes data (Fig. 6a). This problem is solved by both TDIET and QUAKE and the time history of the horizontal hydrodynamic force on the cylinder is compared (Fig. 6b; the geometry is shown in the figure). Both methods respond in a very similar way to the seismic acceleration. The crude approximation used to derive QUAKE is probably responsible for the numerical discrepancy between the two results.

As was earlier remarked, the convolution operator in QUAKE makes it extremely expensive for long time calculations, e.g. a computation of hydrodynamic forces due to an earthquake with a duration of 50 seconds by TDIET, is about 600 times faster than the corresponding computation by QUAKE (using the same number of time steps and a similar spacial partition).

Acknowledgement

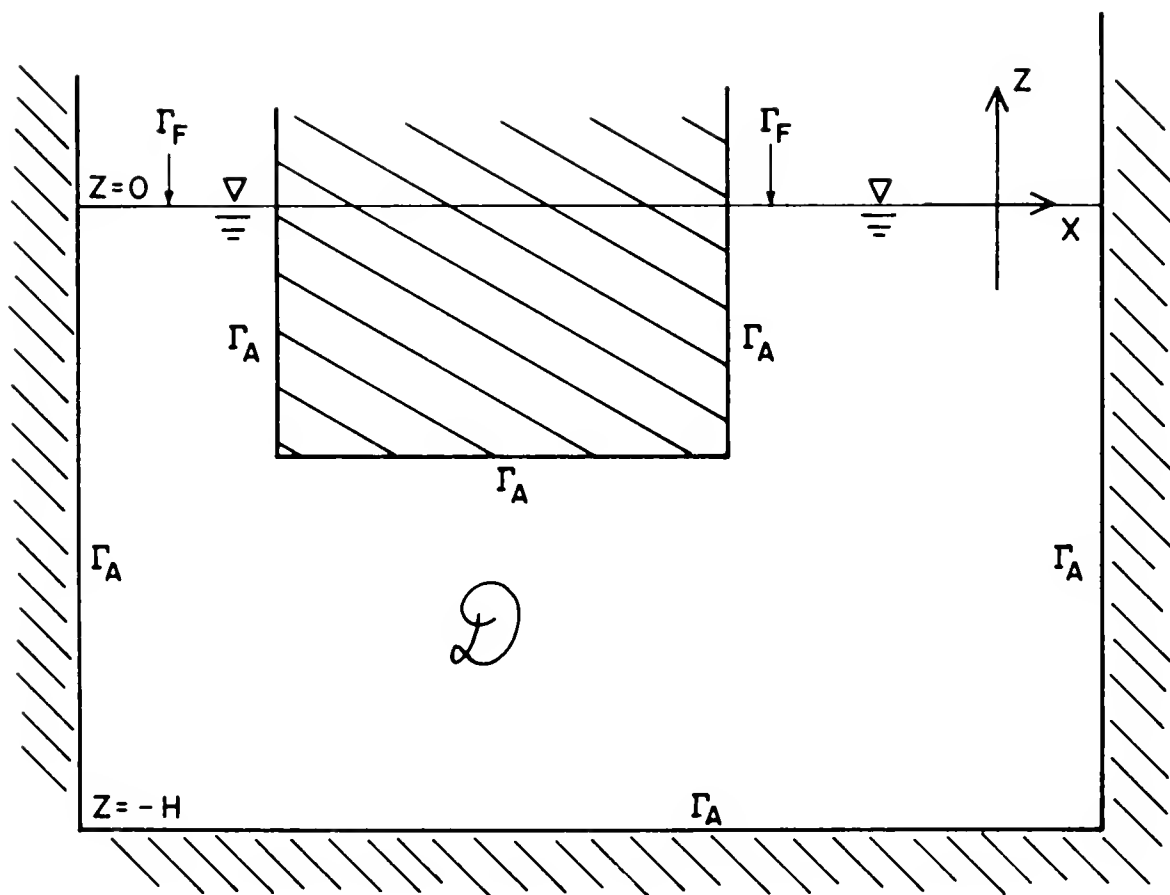
We thank Prof. S. Z. Burstein for critically reading this manuscript. We thank Mr. H. Bonze from Frederic R. Harris, Inc. for suggesting this problem and for many helpful discussions concerning the engineering applications of these methods.

References

1. R. K. Chan and C. W. Hirt, "Two-Dimensional Calculations of the Motion of Floating Bodies", Proceedings of the 10th Hydrodynamic Symposium, June 1974, M.I.T., Massachusetts.
2. A. B. Finkelstein, "The Initial Value Problem for Transient Water Waves", Comm. Pure Appl. Math., Vol. 10, 1957.
3. R. T. Ho and A. Harten, "On Green's Function Techniques for Solutions of Floating Body Problems", Proceedings of Ocean Engineering III, June 1975, University of Delaware.
4. J. J. Stoker, "Water Waves", Interscience Publishers, Inc., New York, 1957.
5. J. V. Wehausen, "The Motion of Floating Bodies", Annual Review of Fluid Mechanics, Vol. 3, 1971, pp. 237-268.

Table 1: Comparison between numerical solution
and exact solution in Example 1.

I	$\phi_{\text{numerical}}$	ϕ_{exact}	$Z_{\text{numerical}}$	Z_{exact}
1	-18.931	-18.794	-.0352	-.0284
2	-17.979	-17.880	-.0335	-.0408
3	-15.521	-15.473	-.0244	-.0195
4	-12.082	-11.997	-.0126	-.0116
5	- 8.284	- 8.259	-.0161	-.0194
6	- 4.321	- 4.315	-.0179	-.0172
7	0.000	0.000	.0000	.0000
8	4.321	4.315	.0179	.0172
9	8.284	8.259	.0161	.0194
10	12.082	11.997	.0126	.0116
11	15.521	15.478	.0244	.0195
12	17.979	17.880	.0335	.0408
13	18.931	18.794	.0352	.0284
14	17.979	17.880	.0335	.0408
15	15.521	15.478	.0244	.0195
16	12.082	11.997	.0126	.0116
17	8.284	8.259	.0161	.0194
18	4.321	4.315	.0179	.0172
19	0.000	0.000	.0000	.0000
20	- 4.321	- 4.315	-.0179	-.0172
21	- 8.284	- 8.259	-.0161	-.0194
22	-12.082	-11.997	-.0126	-.0116
23	-15.521	-15.478	-.0244	-.0195
24	-17.979	-17.880	-.0335	-.0408
25	-18.931	-18.794	-.0352	-.0284



$$\Gamma = \Gamma_A + \Gamma_F$$

FIGURE 1

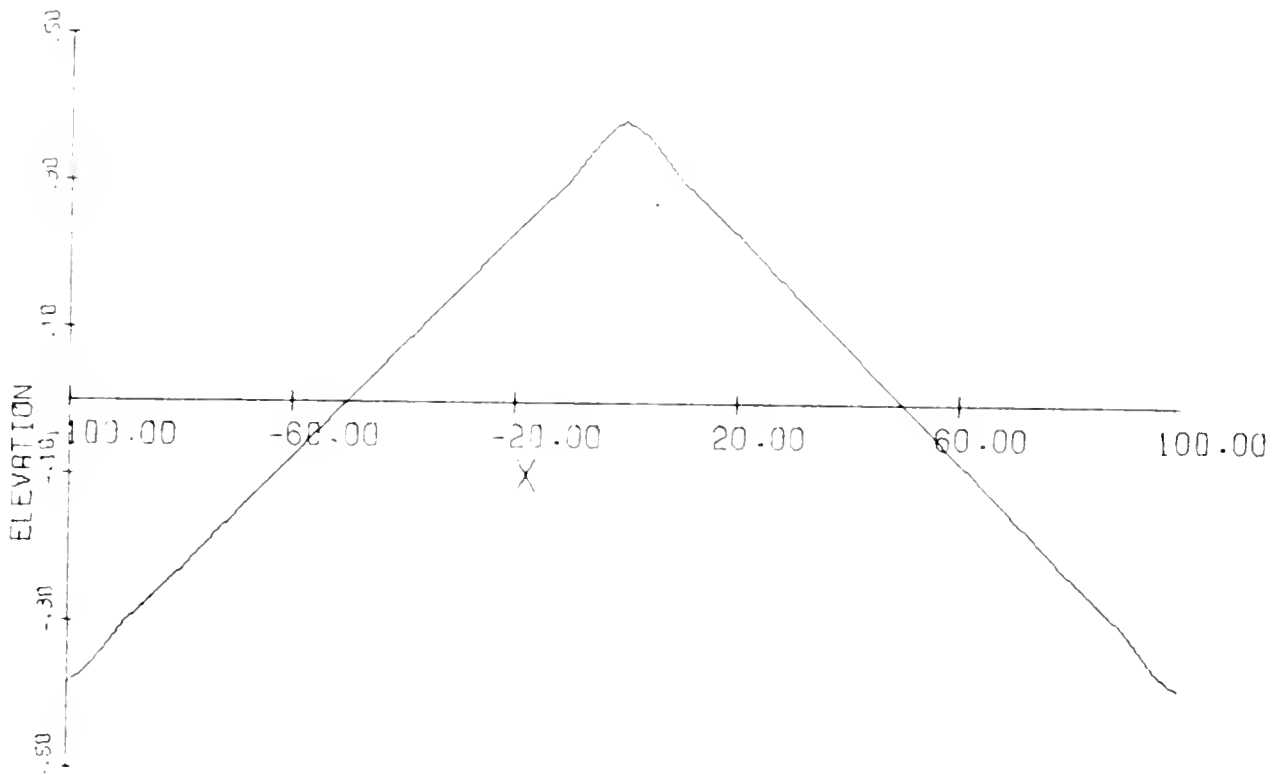


Figure 2a: Initial surface elevation (Example 1).

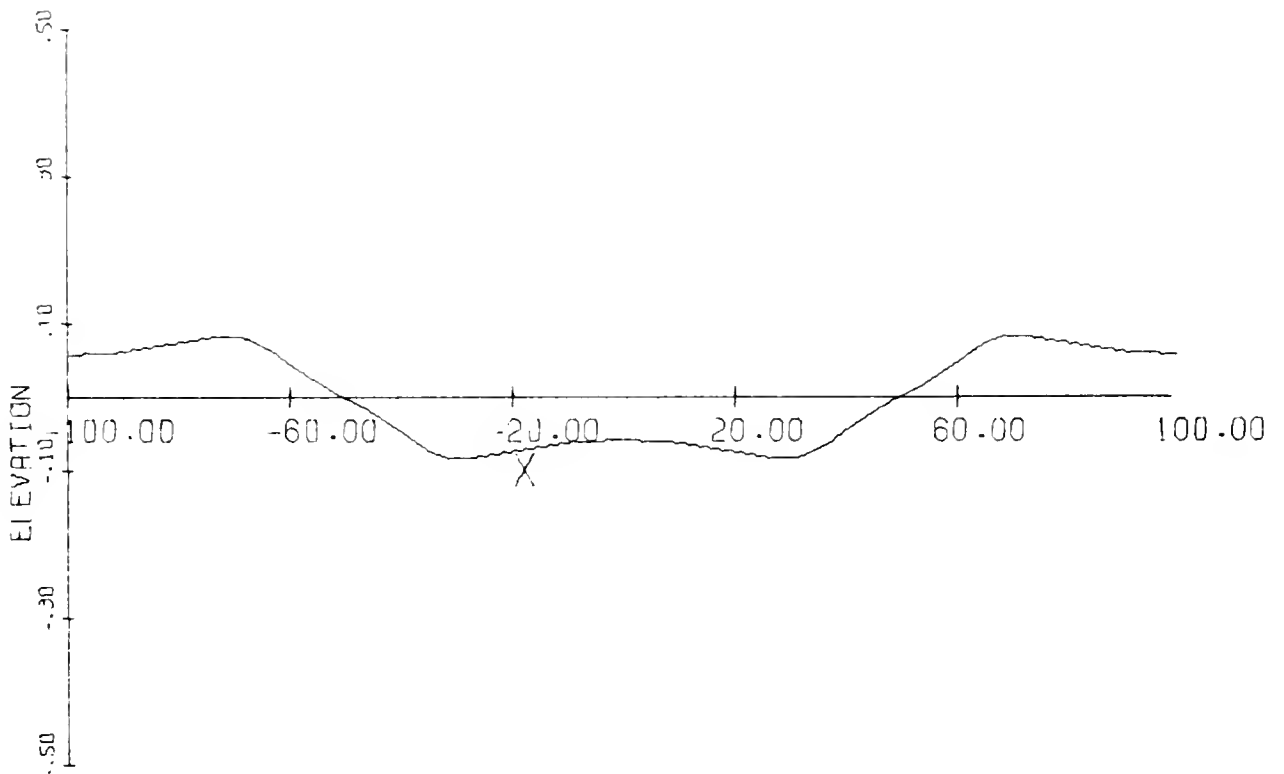


Figure 2b: Surface elevation at $t = 8$ (Example 1).

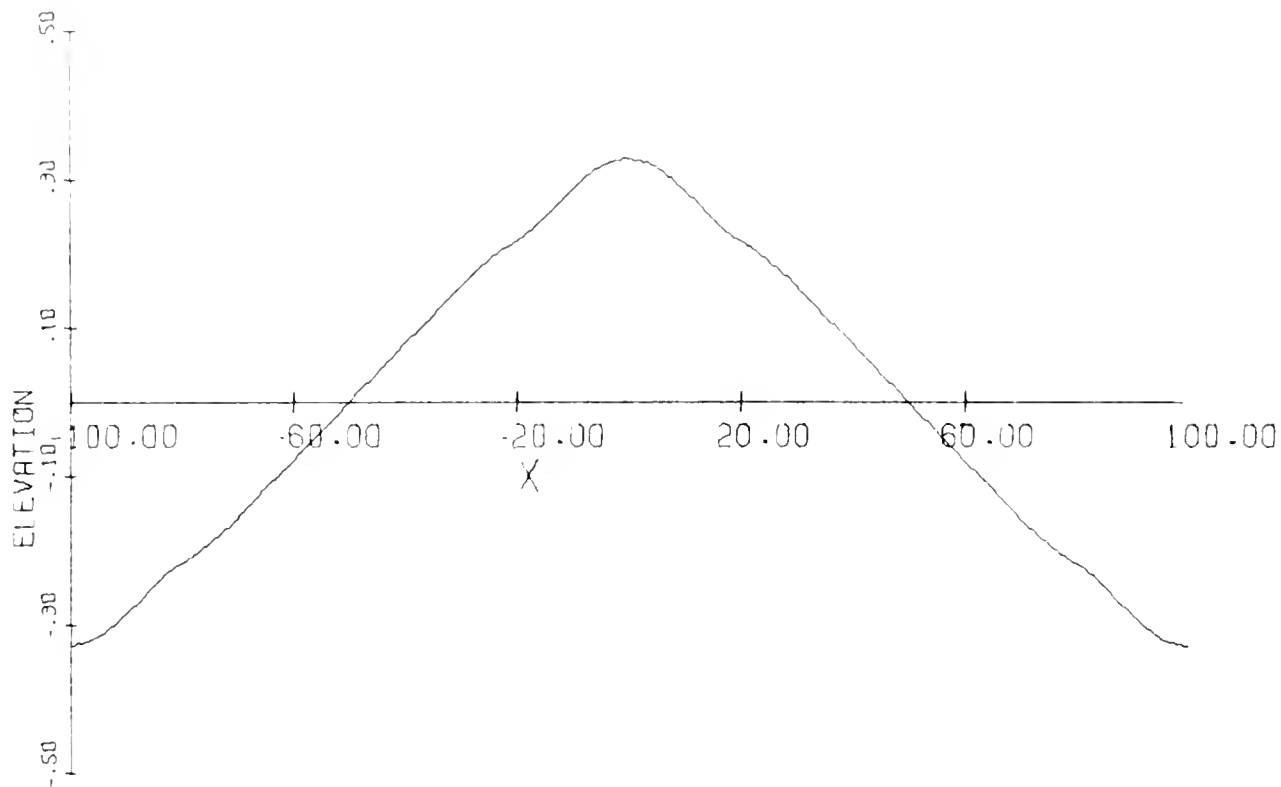


Figure 2c: Surface elevation at $t = 12$ (Example 1).

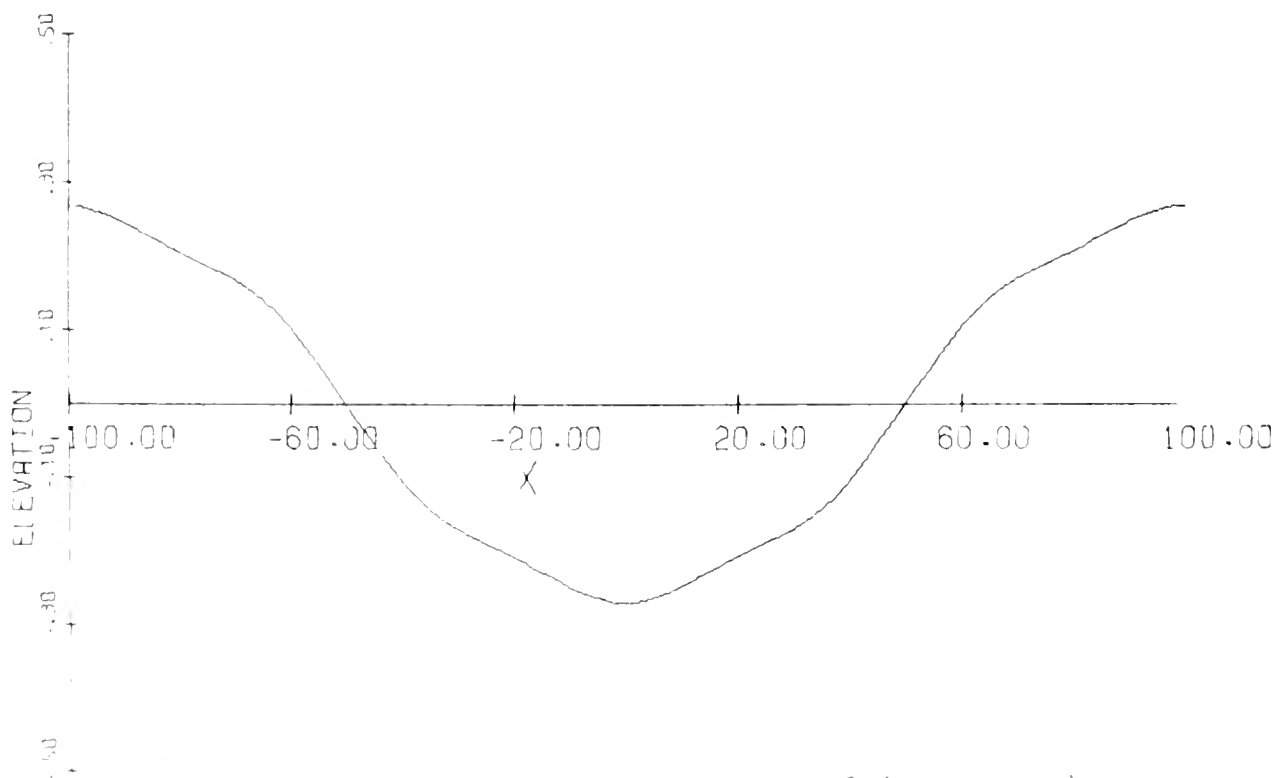


Figure 2d: Surface elevation at $t = 16$ (Example 1).

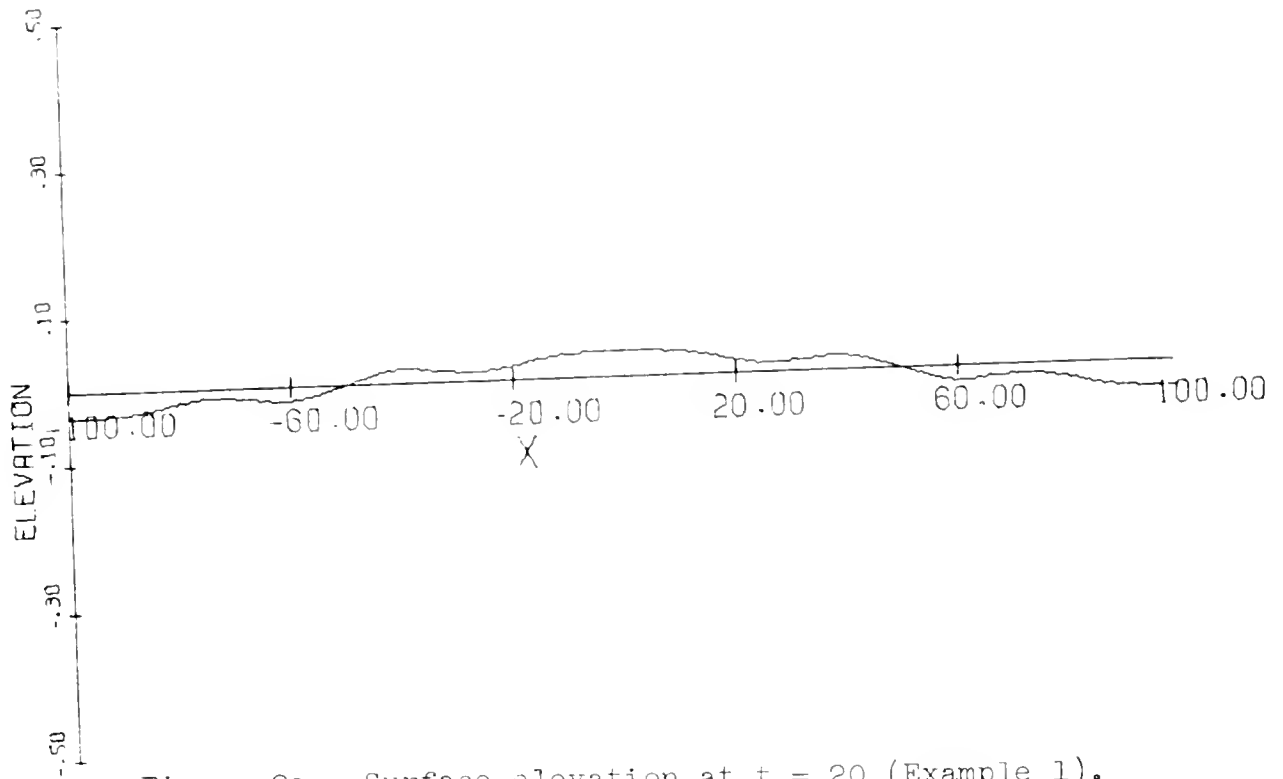


Figure 2e: Surface elevation at $t = 20$ (Example 1).

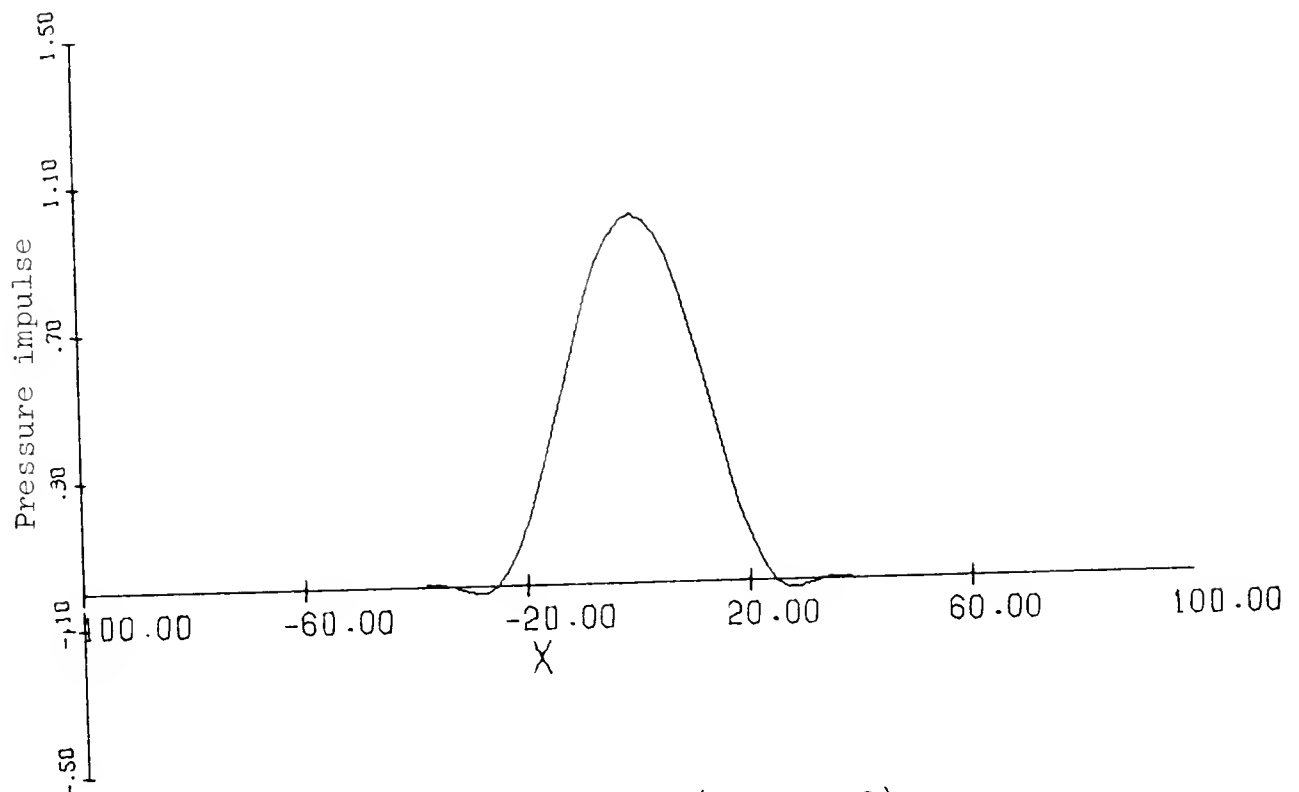


Figure 3a: Pressure impulse (Example 2).

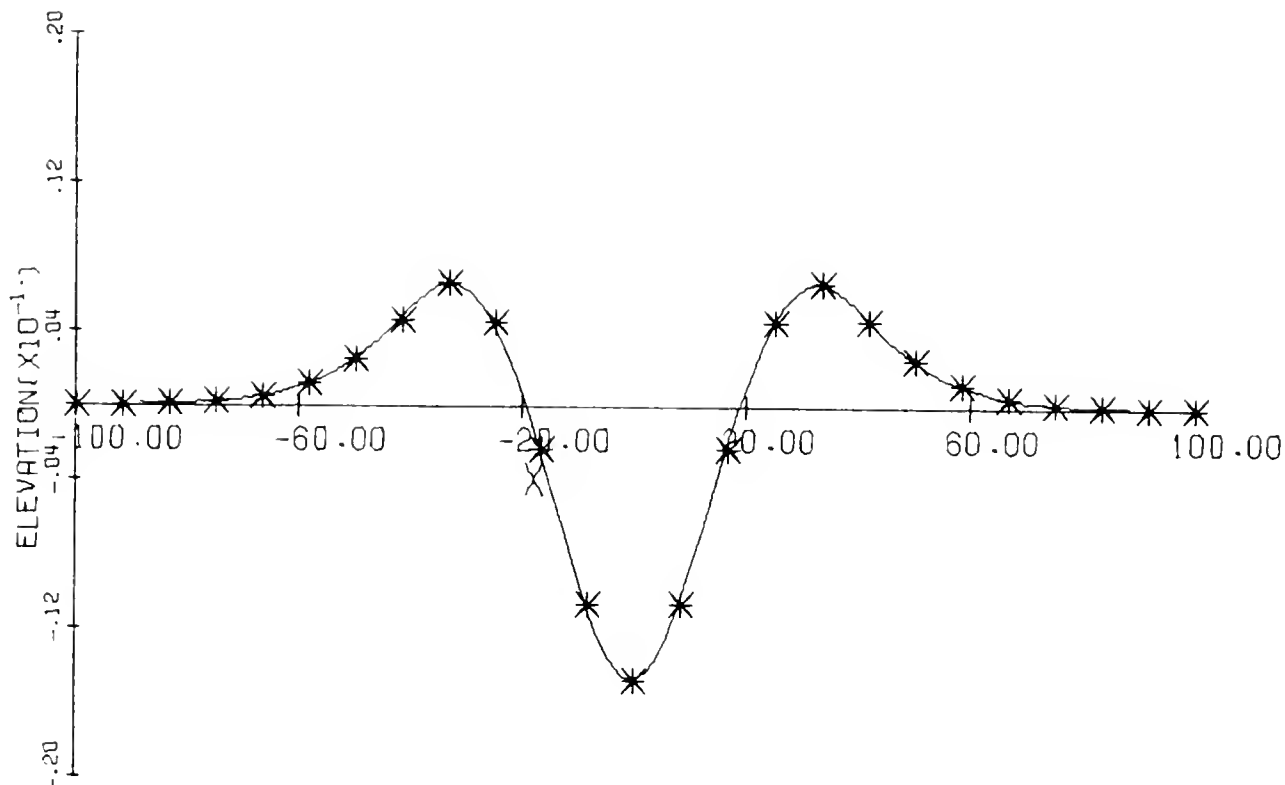


Figure 3b: Surface elevation at $t = 2.5$ (Example 2).

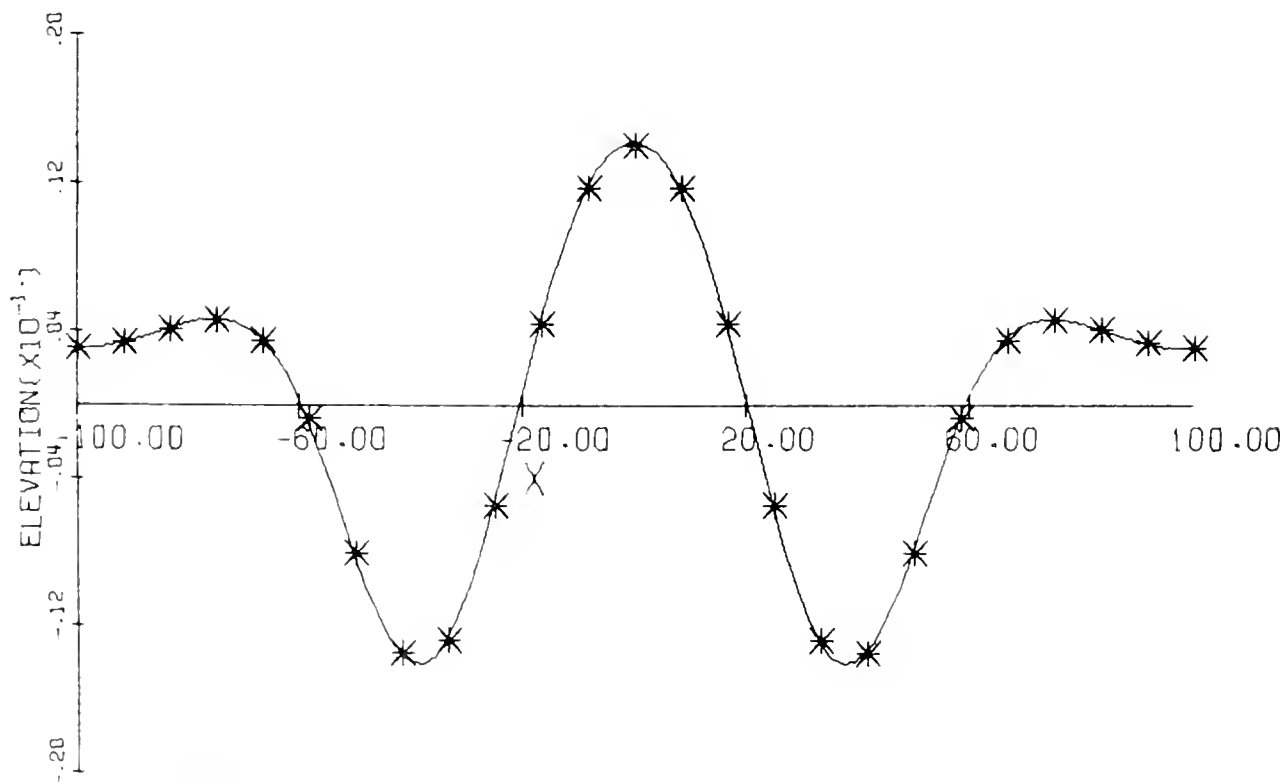


Figure 3c: Surface elevation at $t = 5$ (Example 2).

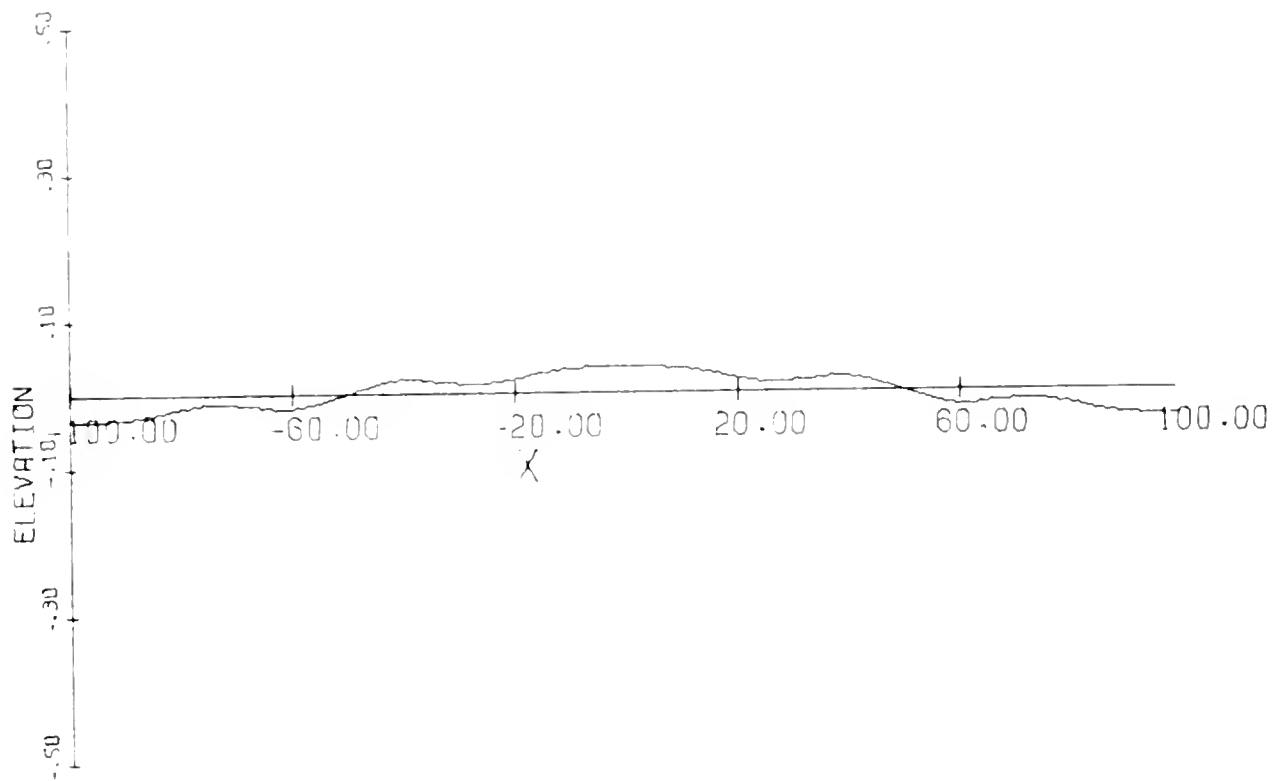


Figure 2e: Surface elevation at $t = 20$ (Example 1).

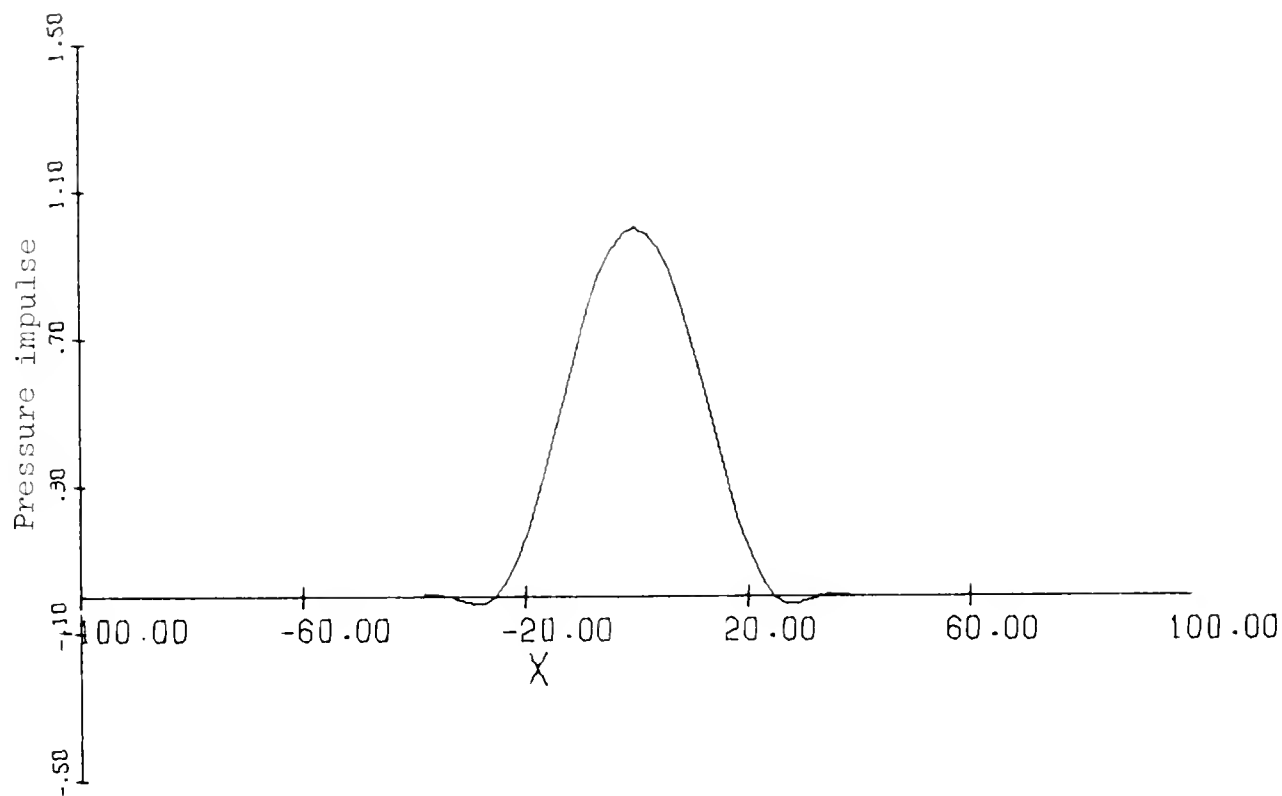


Figure 3a: Pressure impulse (Example 2).

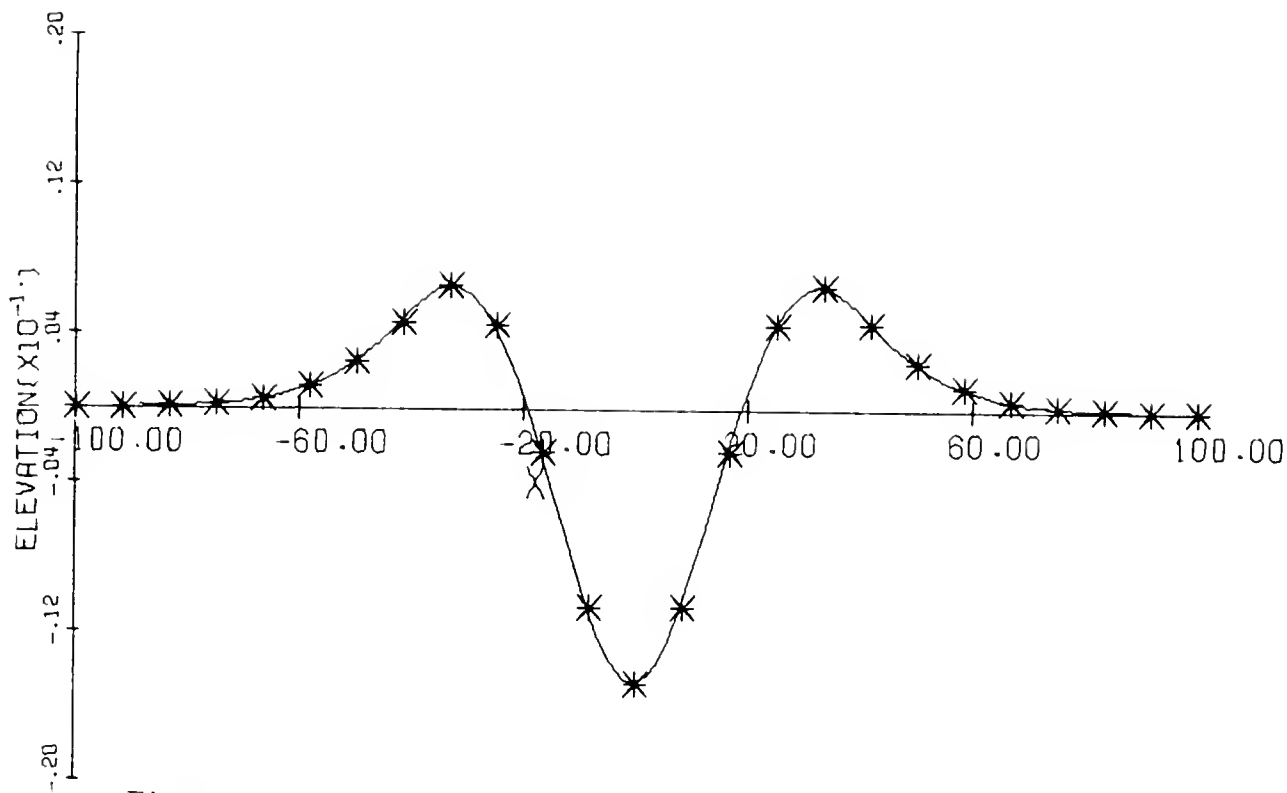


Figure 3b: Surface elevation at $t = 2.5$ (Example 2).

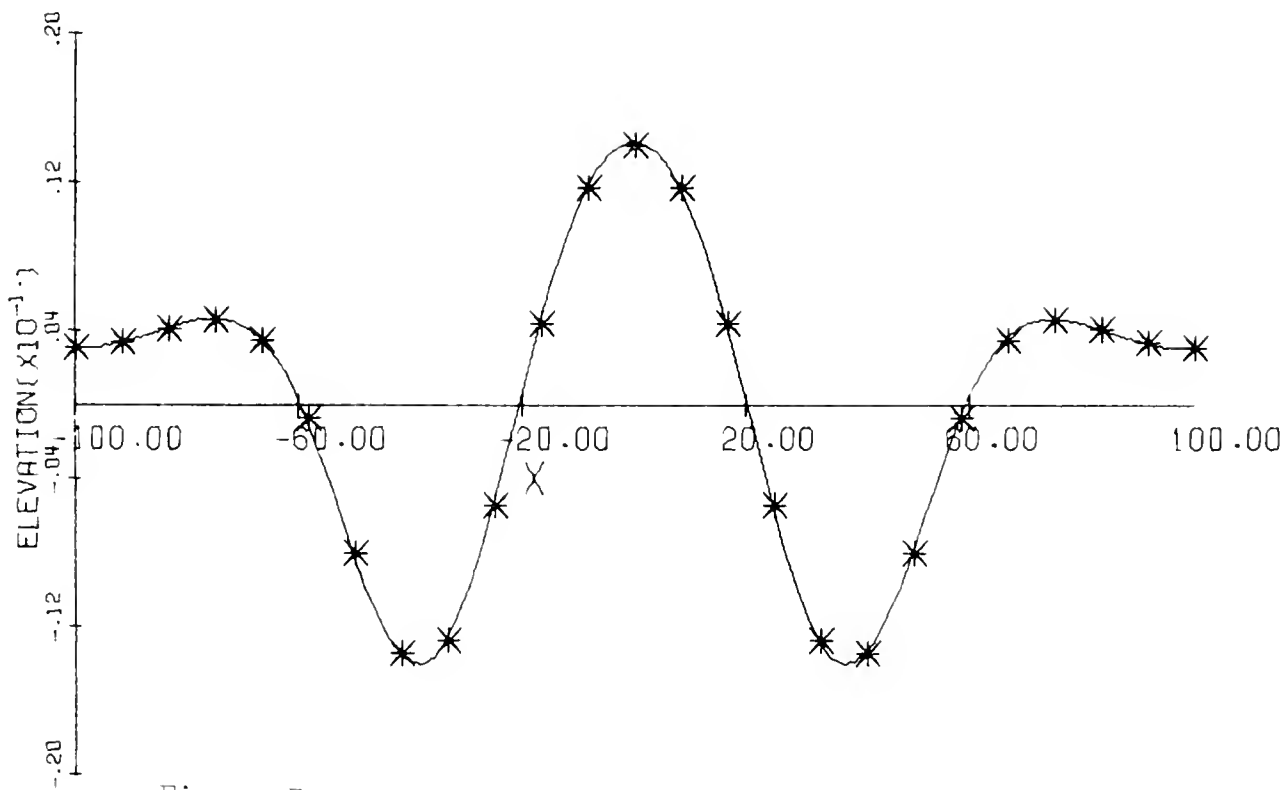


Figure 3c: Surface elevation at $t = 5$ (Example 2).

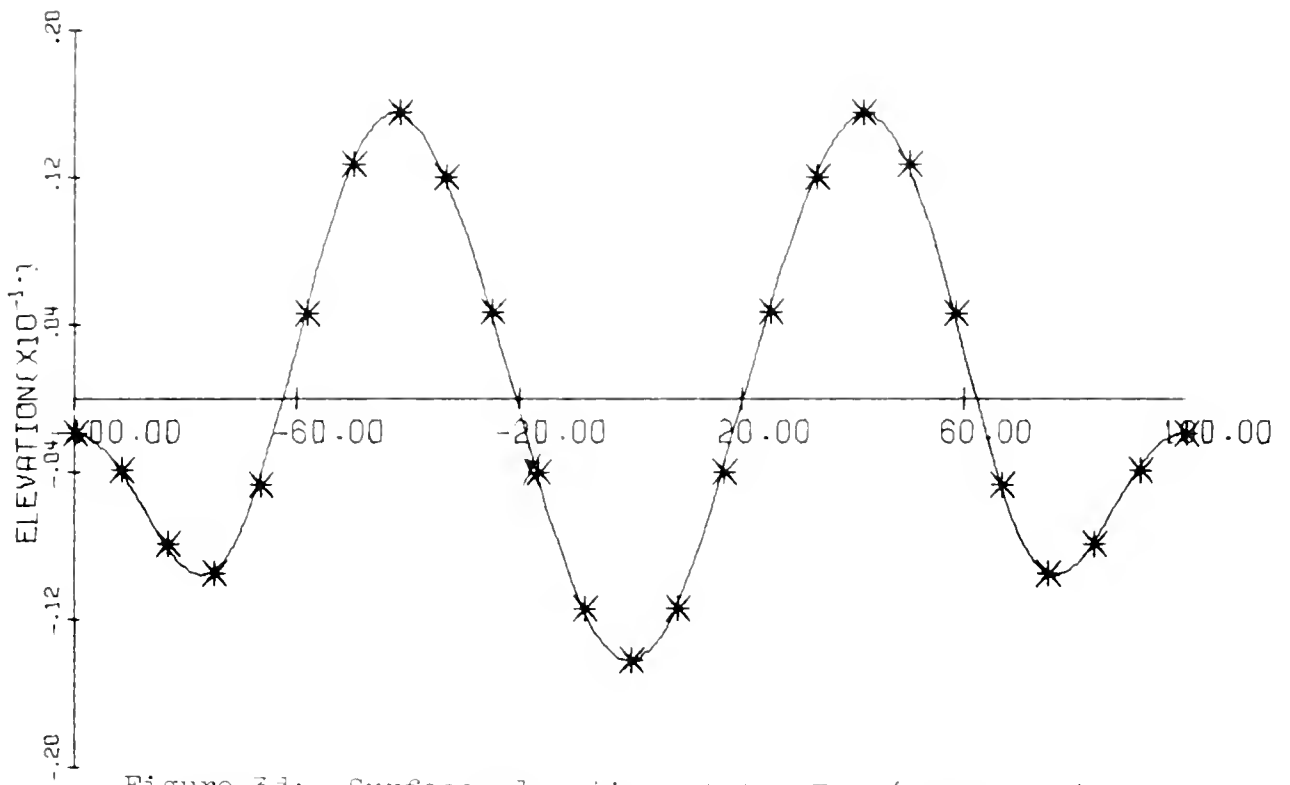


Figure 3d: Surface elevation at $t = 7.5$ (Example 2).

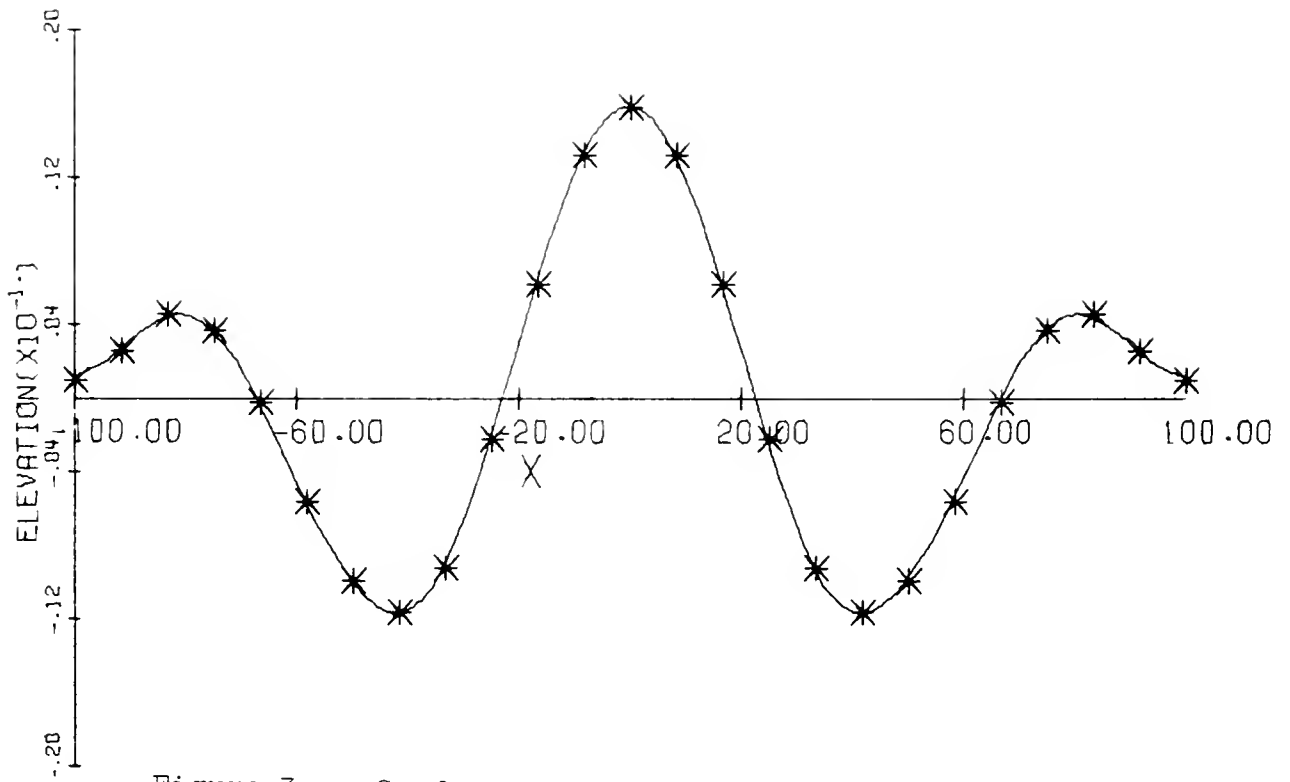


Figure 3e: Surface elevation at $t = 10$ (Example 2).

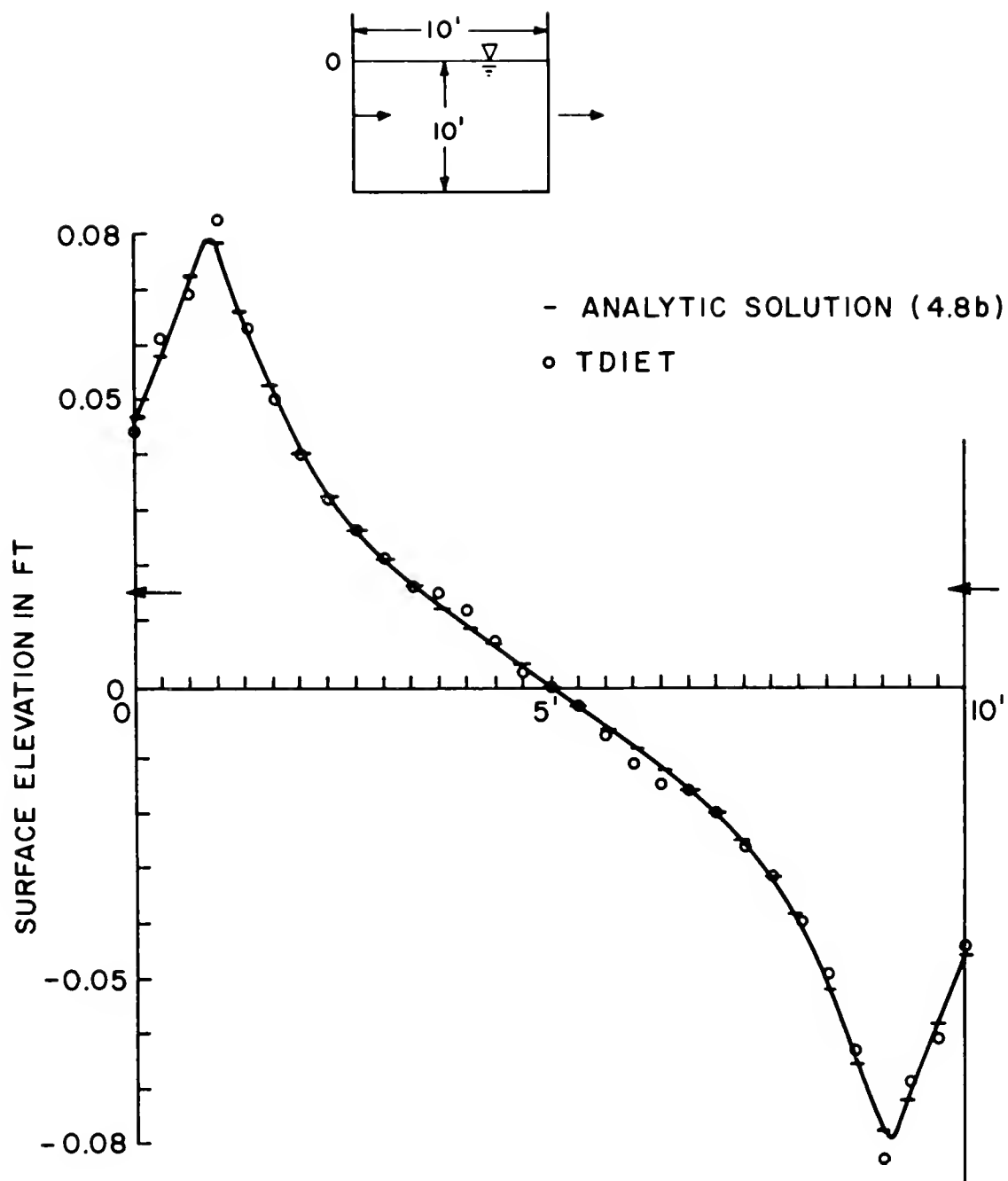


FIGURE 4 SURFACE ELEVATION AT $t = 0.75$ SEC

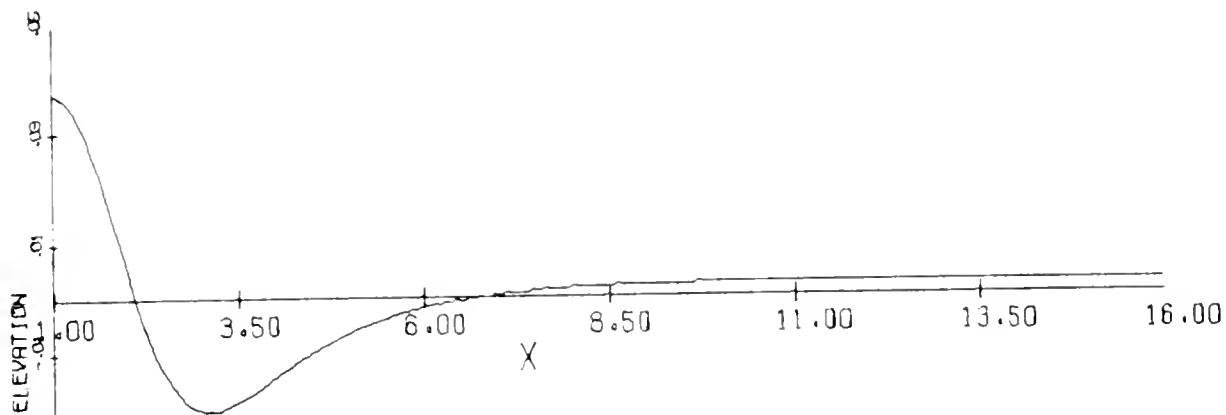


Figure 5a: Free surface profile at the end of one oscillation (Heaving cylinder).

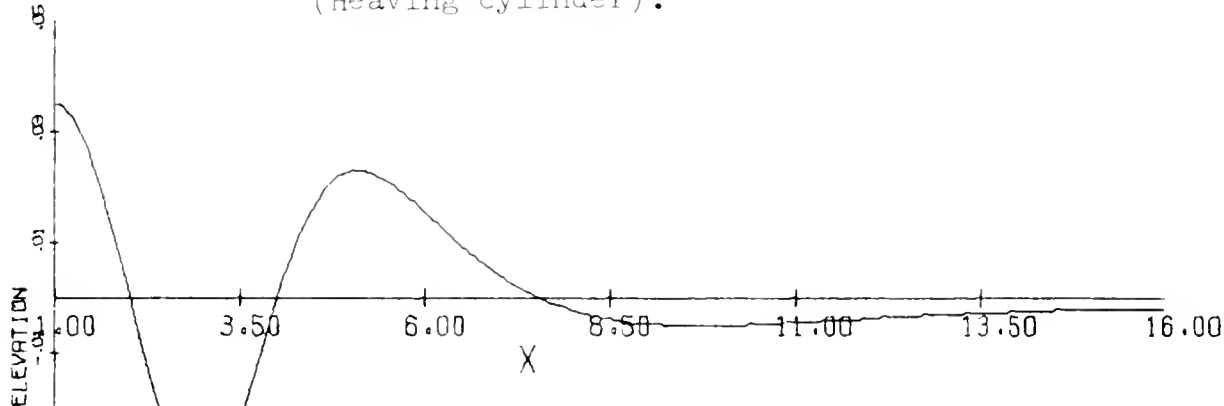


Figure 5b: Free surface profile at the end of two oscillations (Heaving cylinder).

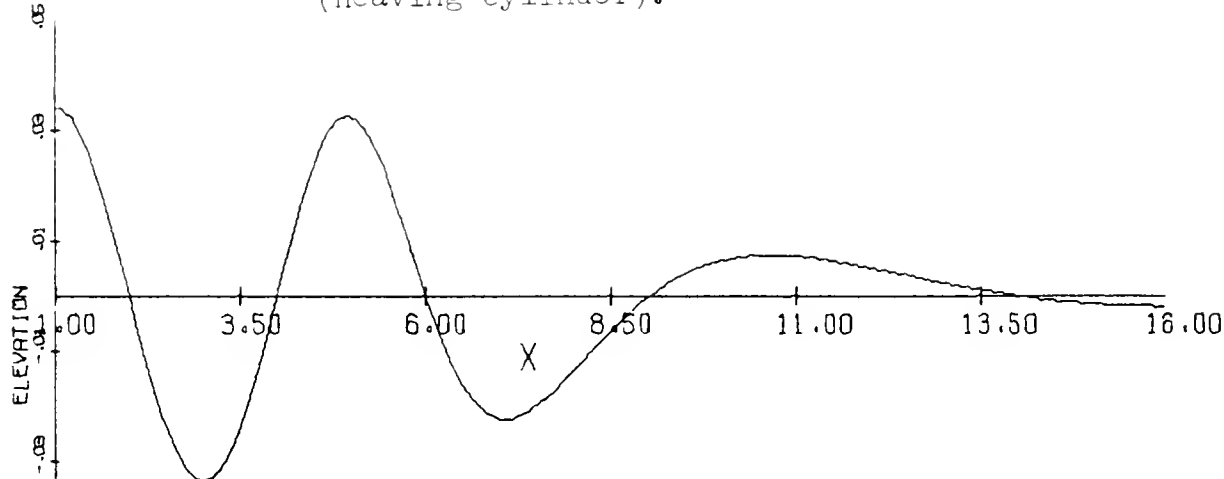


Figure 5c: Free surface profile at the end of three oscillations (Heaving cylinder).

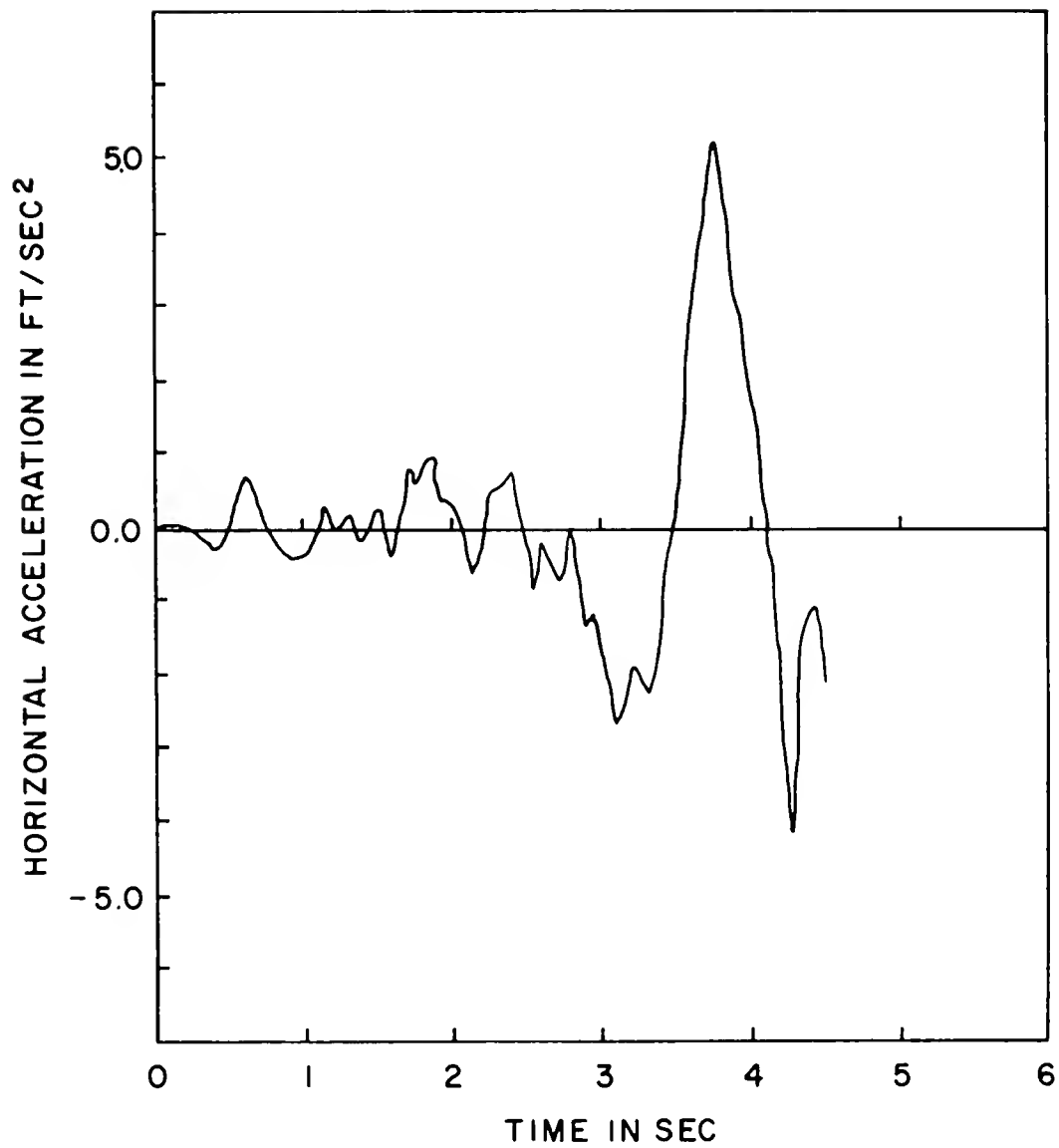


FIGURE 6a HORIZONTAL SEISMIC ACCELERATION AT WALLS

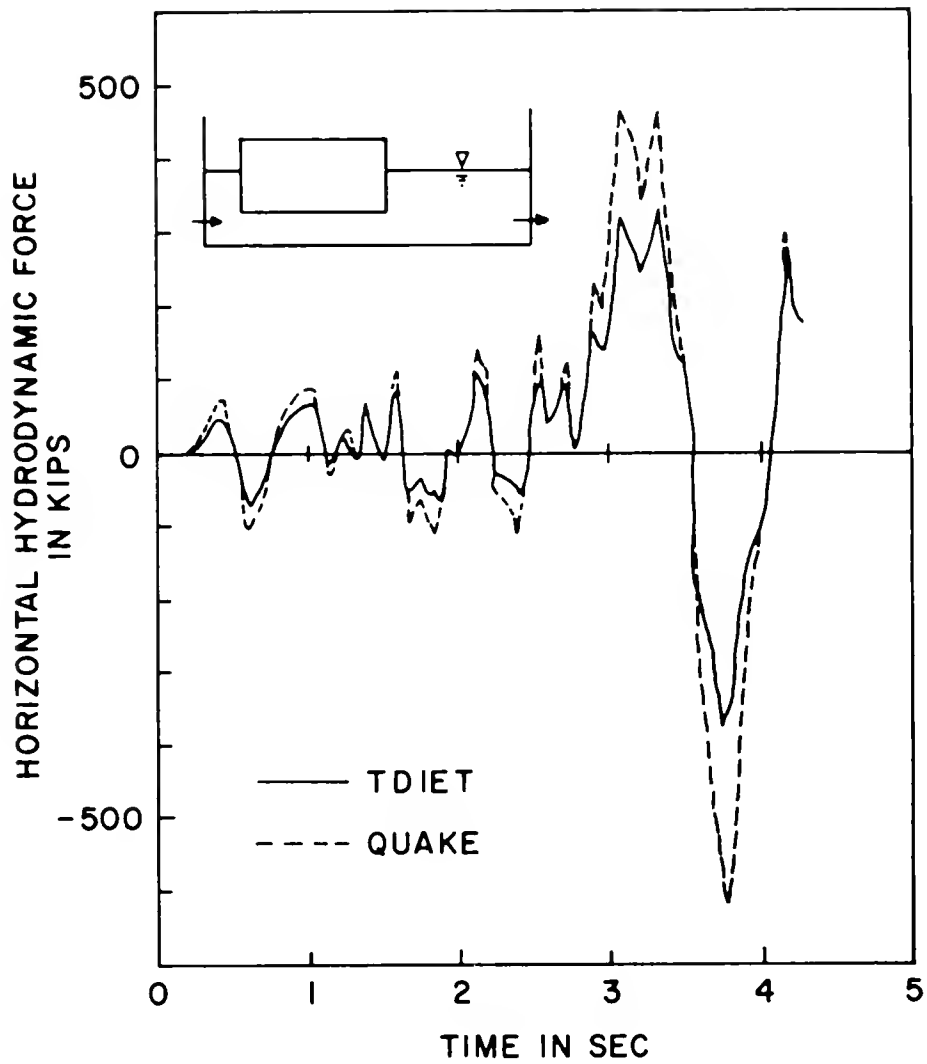


FIGURE 6b HORIZONTAL HYDRODYNAMIC FORCE ON BODY INDUCED BY AN EARTHQUAKE.

This report was prepared as an account of Government sponsored work. Neither the United States, nor the Administration, nor any person acting on behalf of the Administration:

- A. Makes any warranty or representation, express or implied, with respect to the accuracy, completeness, or usefulness of the information contained in this report, or that the use of any information, apparatus, method, or process disclosed in this report may not infringe privately owned rights; or
- B. Assumes any liabilities with respect to the use of, or for damages resulting from the use of any information, apparatus, method, or process disclosed in this report.

As used in the above, "person acting on behalf of the Administration" includes any employee or contractor of the Administration, or employee of such contractor, to the extent that such employee or contractor of the Administration, or employee of such contractor prepares, disseminates, or provides access to, any information pursuant to his employment or contract with the Administration, or his employment with such contractor.

